



**ESKİŞEHİR TEKNİK ÜNİVERSİTESİ**  
ESKİŞEHİR TECHNICAL UNIVERSITY



**Materials Science and Engineering**

**MLZ 447**  
***Materials Processing***  
***Laboratory-II***

**2024-2025**  
***Fall Semester***

**Course Instructors**

Prof. Dr. Gürsoy ARSLAN  
Prof. Dr. A. Tuğrul SEYHAN  
Prof. Dr. Cemail AKSEL  
Assist. Prof. Dr. G. İpek SELİMOĞLU  
Assist. Prof. Dr. H. Boğaç POYRAZ  
Res. Assist. Dr. S. Çağrı ÖZER

**Course Coordinator**

Res. Assist. Dr. S. Çağrı ÖZER

**Laboratory Instructors**

Res. Assist. Dr. S. Çağrı ÖZER  
Res. Assist. Dr. Kübra GÜRCAN BAYRAK  
Res. Assist. Dr. Levent KÖROĞLU  
Res. Assist. Dr. Enes İ. DÜDEN  
Res. Assist. Ö. Başak ÖZKAN KOLCUBAŞI  
Res. Assist. Ertuğrul İŞLEK  
Res. Assist. Emine ERSEZER  
Res. Assist. Gülseda ŞENEL  
Lec. Ramazan KALE  
Lec. Tuğba Burçin ULUDAĞ

# MLZ 447

## Materials Processing Laboratory-II

### Course Instructors:

MLZ 447 A	Prof. Dr. Gürsoy ARSLAN
MLZ 447 B	Prof. Dr. Cemal AKSEL
MLZ 447 C	Prof. Dr. A. Tuğrul SEYHAN
MLZ 447 D	Assist. Prof. Dr. H. Boğaç POYRAZ
MLZ 447 E	Assist. Prof. Dr. G. İpek SELİMOĞLU
MLZ 447 F	Res. Assist. Dr. S. Çağrı ÖZER

### Lab. Groups & Hours:

Group A	: Monday	14:00-16:00
Group B	: Tuesday	09:00-11:00
Group C	: Thursday	16:00-18:00
Group D	: Wednesday	15:00-17:00
Group E	: Thursday	11:00-13:00
Group F	: Tuesday	14:00-16:00

### GRADING TABLE

Exam	Exam Type	Percentage of Exam
<b>QUIZ</b>	<b><u>7</u> Pre-Lab. Quizzes</b> (Exp#1, Exp#2, Exp#3, Exp#4, Exp#5, Exp#6 and Exp#7)	<b>30 %</b>
<b>MIDTERM</b>	<b><u>1</u> Lab. Exam</b>	<b>25 %</b>
<b>FINAL</b>	<b><u>7</u> Reports</b> (Exp#1, Exp#2, Exp#3, Exp#4, Exp#5, Exp#6 and Exp#7)	<b>45 %</b>

**! IMPORTANT NOTE:** Minimum qualifying grade in this course is **50**.

	<b>Experiment</b>	<b>Location</b>	<b>Instructors</b>
<b>EXP #1</b>	Cold-Rolling	MatSE Metallic Processes Lab. MLZ 119	Res. Assist. Dr. S. Çağrı ÖZER Res. Assist. Gülseda ŞENEL
<b>EXP #2</b>	a) Jominy End-Quench Test	MatSE Furnace Lab. MLZ 116	Res. Assist. Dr. Kübra GÜRCAN BAYRAK Res. Assist. Ö. Başak ÖZKAN KOLCUBAŞI
	b) Hardness Testing Techniques	MatSE Ceramography Lab. MLZ 118	
<b>EXP #3</b>	a) Heat Treatment of Steels	MatSE Furnace Lab. MLZ 116	Res. Assist. Emine ERSEZER Res. Assist. Gülseda ŞENEL
	b) Microstructure Analysis in Metallic Materials	MatSE Metallic Processes Lab. MLZ 119	
<b>EXP #4</b>	OES Spectrometer	MatSE Metallic Processes Lab. MLZ 119	Res. Assist. Ertuğrul İŞLEK
<b>EXP #5</b>	a) Polymer Processing	MatSE Polymer Lab. MLZ 130	Res. Assist. Dr. Levent KÖROĞLU
	b) Thermal Characterization of Polymeric Materials	MatSE Polymer Lab. MLZ 130	Res. Assist. Dr. Levent KÖROĞLU
<b>EXP #6</b>	Thin Film Deposition and Characterization	MatSE Thin Film Lab. MLZ 129	Res. Assist. Dr. Enes İ. DÜDEN Res. Assist. Ö. Başak ÖZKAN KOLCUBAŞI
<b>EXP #7</b>	a) Fatigue-Charpy Impact-Tension Testing	Faculty of Aeronautics and Astronautics A Block, Materials Lab.	Lec. Ramazan KALE Res. Assist. Ertuğrul İŞLEK
	b) NDT Experiments		Lec. Tuğba Burçin ULUDAĞ Res. Assist. Ertuğrul İŞLEK

## SCHEDULE

<b>Lab. Meeting (03.10.2024)</b>		
<b>07.10.2024-11.10.2024</b>	<i>Report Submission Due By</i> <b>14.10.2024-18.10.2024</b>	Cold Rolling
<b>14.10.2024-18.10.2024</b>	<i>Report Submission Due By</i> <b>21.10.2024-25.10.2024</b>	Jominy End-Quench Test Hardness Testing Techniques
<b>21.10.2024-25.10.2024</b>	<i>Report Submission Due By</i> <b>04.11.2024-08.11.2024</b>	Heat Treatment of Steels Microstructure Analysis in Metallic Materials
<b>04.11.2024-08.11.2024</b>	<i>Report Submission Due By</i> <b>25.11.2024-29.11.2024</b>	OES Spectrometer
<b>Midterm Week (09-24 November 2024)</b>		
<b>25.11.2024-29.11.2024</b>	<i>Report Submission Due By</i> <b>02.12.2024-06.12.2024</b>	Polymer Processing Thermal Characterization of Polymeric Materials
<b>02.12.2024-06.12.2024</b>	<i>Report Submission Due By</i> <b>09.12.2024-13.12.2024</b>	Thin Film Deposition and Characterization
<b>09.12.2024-13.12.2024</b>	<i>Report Submission Due By</i> <b>16.12.2024-20.12.2024</b>	Fatigue-Charpy Impact-Tension Tests
<b>16.12.2024-20.12.2024</b>	<i>Report Submission Due By</i> <b>23.12.2024-27.12.2024</b>	NDT Experiments
<b>“LAB. EXAM” (Not confirmed, to be announced later) Final Week (02-15 January 2024)</b>		

**GENERAL INSTRUCTIONS FOR  
MLZ 447 MATERIALS PROCESSING LABORATORY-II**

1. It is **extremely important** that you read each experiment and basic references as well as watch the video of experiments prior to the lab. (Link of the video playlist: <https://www.youtube.com/playlist?list=PLQUb7RtOnw8KR8KgcPrbM8iu7jnc083SO>). The lab instructor will ask general questions during the lab to test your understanding of the lab.
2. It is obligatory to **wear laboratory apron** unless the lab instructor tells otherwise. Students without aprons (lab coats) will not be admitted to the laboratory.
3. The lab groups must be **present in the room/building** where the lab will take place (stated in the lab manual) **5 minutes before the lab** starts. Students are obliged to learn the location of the labs before the labs begin.
4. All labs will be evaluated with a quiz and a report. It's definitely obligatory to **have the lab. manual** with you and **read the corresponding lab. chapter** before coming to the lab.
5. **Before each lab.** starts, there will be a **quiz composed of 1-3 questions**. If student fails from the quiz (**min. 50/100**), he/she neither can attend the lab. nor submit the lab. report regarding that lab.
6. Students are responsible to **submit the lab reports** to turnitin.com the **following week until 17:00** as a PDF file. The lab instructor will grade the lab. reports within a week and will post the results. If you wish to discuss the grade, make an appointment to see the lab instructor at his/her convenience.
7. The nature of working in groups implies that there should be cooperation and discussion between members of the group and the lab instructor. It is, however, expected that when students prepare their reports, that they do so individually using their own words and interpretation. **Plagiarizing/blatant copying of a report or reference and utilizing AI** will result in an automatic zero for that lab for the first offense. A second offense will result in an automatic **FF grade** for the course.

8. **Students must attend each lab on the specified group.** The students will be admitted to the class within the first half an hour. Lab reports must be handed in on time; otherwise 10% will be deducted from the mark for each day late.

9. **Minimum qualifying grade** for this course is determined as **50**.

10. **Lab. manuals** will be available on the department web-site: <http://matse.eskisehir.edu.tr>

11. **Instructions for Informal Lab Reports:** Each experiment should be organized in the report neatly and carefully as given below;

- I. A **Cover Page** with “Student Name”, “Student ID Number”, “Lab. Group” and “Experiment Name”.
- II. An **Introduction** section that briefly introduces the concepts of each lab.
- III. **Equipment & Materials** which were used in the experiment.
- IV. An **Experimental Procedure** section that carefully summarizes the method used in each experiment.
- V. A **Results & Discussion** section, as instructed by each lab instructor.
- VI. **References** (APA etc. style, complete citation)

The reports must be written ***in English*** and will be prepared using a computer. This will be announced by the lab instructor at the end of each experiment.

*\*The requests of the lab instructors may be different from what is written in “General Instructions”. In that case, the reports will be prepared according to the requests of the lab instructors.*

## Experiment # 1: Cold-Rolling

**Objective:** Investigating the plastic deformation behavior and the progression of the microstructure of metal and/or metallic alloy slabs during cold-rolling.

**Materials:** Metal Slab

**Equipment:** Rolling Mill

### Background:

Rolling is a plastic deformation process in which metals are passed through a couple (or more) rolls to reduce the thickness. A simple schematic of rolling process is given at Figure 1.



**Figure 1.** Rolling Process

Rolling is classified according to the temperature of the metal rolled; it is classified as “hot rolling” if the temperature of the metal is above its recrystallization temperature, and if the temperature of the metal is below its recrystallization temperature, the process is known as cold rolling.

Cast metal ingots are pre-shaped into various intermediate shapes than plastically deformed to desired products as seen on Figure 2. Typically, a bloom has a square cross section of 150/150 mm or more, slab has a square cross section of 40/250 mm or more and billet has a square cross section of 40/40 mm or more.

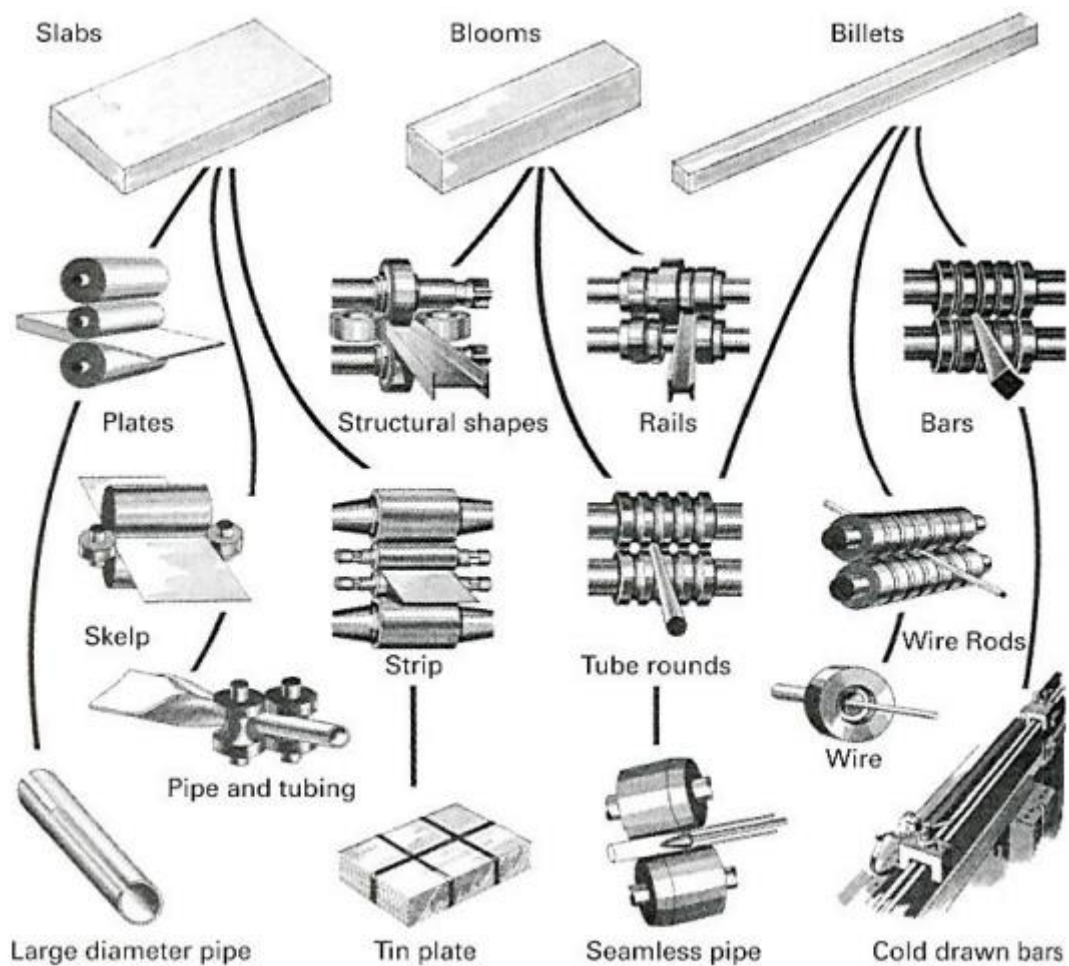


**Figure 2.** Intermediate and final metal shapes of rolling.

Deformation of the material is achieved by radial compression stresses due to the squeezing of metal by rolls and surface shear stresses due to friction between metal and rolls. Metals thickness is reduced while its width and length are increased. Forces affecting the rolling process are given in Figure 3, where  $h_0$  is the thickness before rolling,  $h_1$  is the thickness after rolling,  $v_0$  is the metals entry speed,  $v_1$  is the metals exit speed,  $L$  is the contact length,  $\alpha$  is the contact angle,  $R$  is the roll radius,  $P_r$  is the radial compression force, and  $F$  is the friction force.



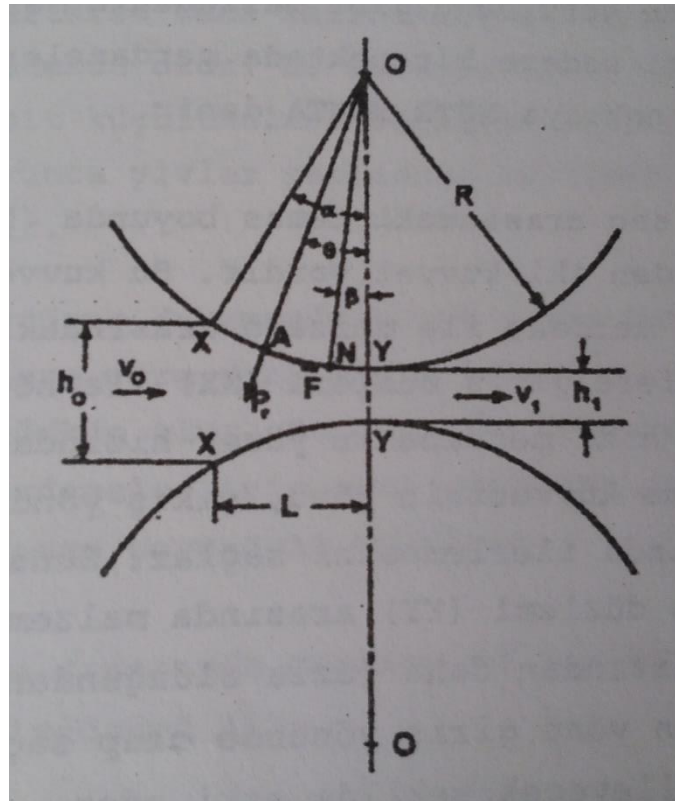


**Figure 3.** Forces in a rolling process.

In order for the metal to move towards the exit,  $F \cdot \cos\alpha$  should be bigger than  $P_r \cdot \sin\alpha$ . ( $P_r \cdot \sin\alpha$  is the horizontal component of compression force and  $F \cdot \cos\alpha$  is the horizontal component of friction force).

The relation between the coefficient of friction  $\mu$  ( $\mu = F/P_r$ ) and the contact angle is given as:

$$F \cos\alpha > P_r \sin\alpha$$

$$F/P_r = \mu > \sin\alpha / \cos\alpha = \tan\alpha$$

$$\mu > \tan\alpha$$

Eq. 1.

In order to identify the parameter that affect the thickness reduction ( $\Delta h$ ), it is necessary to find out the horizontal component of contact surface between the metal and rolls ( $L$ ):

$$L = \left[ R(h_0 - h_1) - \frac{(h_0 - h_1)^2}{4} \right]^{1/2} \approx [R(h_0 - h_1)]^{1/2}$$

$$\Delta h = h_0 - h_1$$

$$L = (R\Delta h)^{1/2} \quad \text{Eq. 2.}$$

$$\tan \alpha = \frac{L}{R-\Delta h/2} = \frac{(R\Delta h)^{1/2}}{R-\Delta h/2} \approx (\Delta h/R)^{1/2} \quad \text{Eq. 3.}$$

Combining equations 1, 2 and 3 would give;

$$(\Delta h)_{max} = \mu^2 R \quad \text{Eq. 4.}$$

From equation 4, it can be seen that the maximum thickness reduction during rolling is related to the friction coefficient and roll radius. Increasing either one or both increases the amount of deformation during the rolling process.

### **Experimental Procedure**

- Measure the thickness and width of the slab samples.
- Place the sample between the rolls and stepwise reduce the thickness.
- Measure the thickness of the slabs after plastic deformation again.
- Calculate the coefficient of friction and reduction in area.

### **References**

1. Kayalı, E.S. and Ensari, C. (2000). *Metallere Plastik Şekil Verme İlke ve Uygulamaları*, 3<sup>rd</sup> ed. İstanbul-İTÜ
2. [http://www.efunda.com/processes/metal\\_processing/cold\\_rolling.cfm](http://www.efunda.com/processes/metal_processing/cold_rolling.cfm)
3. Marinov, *ME 364 Manufacturing Technology Lecture Notes*

## **Experiment # 2: Jominy End-Quench Test, Hardness Testing Techniques**

### **(a) Jominy End-Quench Test**

**Objective:** Understanding the effect of cooling rate on the hardness and formation of hardenability curve of the selected steel sample.

**Materials:** AISI 4140 alloy steel test sample (ASTM A225).

**Equipment:** Box furnace, jominy end quench test apparatus.

### **Background:**

The Jominy End-Quench test is a standard procedure in order to measure hardenability of steel. Hardenability is a term that is used to describe the ability of an alloy to be hardened by the formation of martensite as a result of a given heat treatment.

The hardenability of a steel depends on:

- (1) the composition of the steel
- (2) the austenitic grain size
- (3) the structure of the steel before quenching.

In general hardenability increases with carbon content and with alloy content. The most important factor influencing the maximum hardness that can be obtained is mass of the metal being quenched. In a small section, the heat is extracted quickly, thus exceeding the critical cooling rate of the specific steel and this part would thus be completely martensitic. The critical cooling rate is that rate of cooling which must be exceeded to prevent formation of nonmartensite products. As section size increases, it becomes increasingly difficult to extract the heat fast enough to exceed the critical cooling rate and thus avoid formation of nonmartensitic products. Hardenability of all steels is directly related to critical cooling rates [1].

## Experimental Procedure

AISI 4140 steel test sample prepared according to the ASTM A255 [2] Test Standard (Figure 1). Preheated samples are placed to the test set-up system and then water is sprayed to the sample as shown in Figure 2 for maximum of 10 minutes. After cooling to the room temperature, two flats 180° apart shall be ground to a minimum depth of 0.015 in. (0.38 mm) along the entire length of the bar and Rockwell C hardness measurements made along the length of the bar. Hardness measurements are made for the first 50 mm (2 in.) along each flat for the first 12.8 mm, hardness readings are taken at 1.6-mm intervals, and for the remaining 38.4 mm every 3.2 mm. A hardenability curve is produced when hardness is plotted as a function of position from the quenched end.

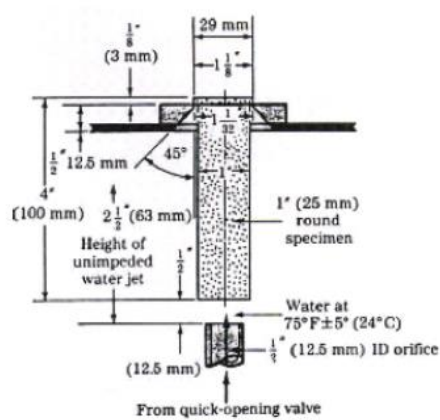


Figure 1. Jominy Test Sample[3]

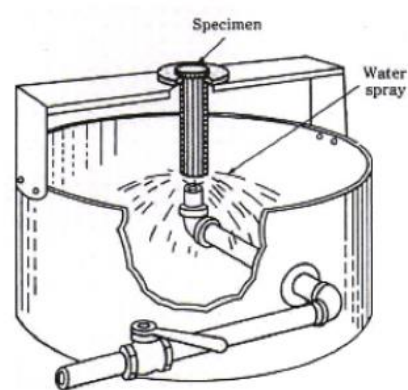


Figure 2. Jominy Test set-up[2]

In a typical hardenability curve [4]; the quenched end is cooled most rapidly and exhibits the maximum hardness, where 100% martensite is the product at this position for most steels. Cooling rate decreases with distance from the quenched end, and the hardness also decreases. With diminishing cooling rate more time is allowed for carbon diffusion and the formation of a greater proportion of the softer pearlite, which may be mixed with martensite and bainite. Thus, a steel that is highly hardenable will retain large hardness values for relatively long distances; a low hardenable one will not. Also, each steel alloy has its own unique hardenability curve.

## REFERENCES

1. <http://web.itu.edu.tr/~arana/jominy.pdf>
2. ASTM A255-10 standard test methods for determining hardenability of steel
3. Shackelford, IF, Introduction to materials science
4. W. D. Callister (2007), Materials Science and Engineering: An Introduction. 7<sup>th</sup> Edition. USA: John Wiley & Sons, Inc.

## **(b) Hardness Testing Techniques**

**Objective:** Investigation of the effects of heat treatment and different cooling conditions by measuring hardness.

**Materials:** AISI 4140 alloy steel heat treated test samples.

**Equipment:** Hardness Test Equipment (EMCOTEST M1).

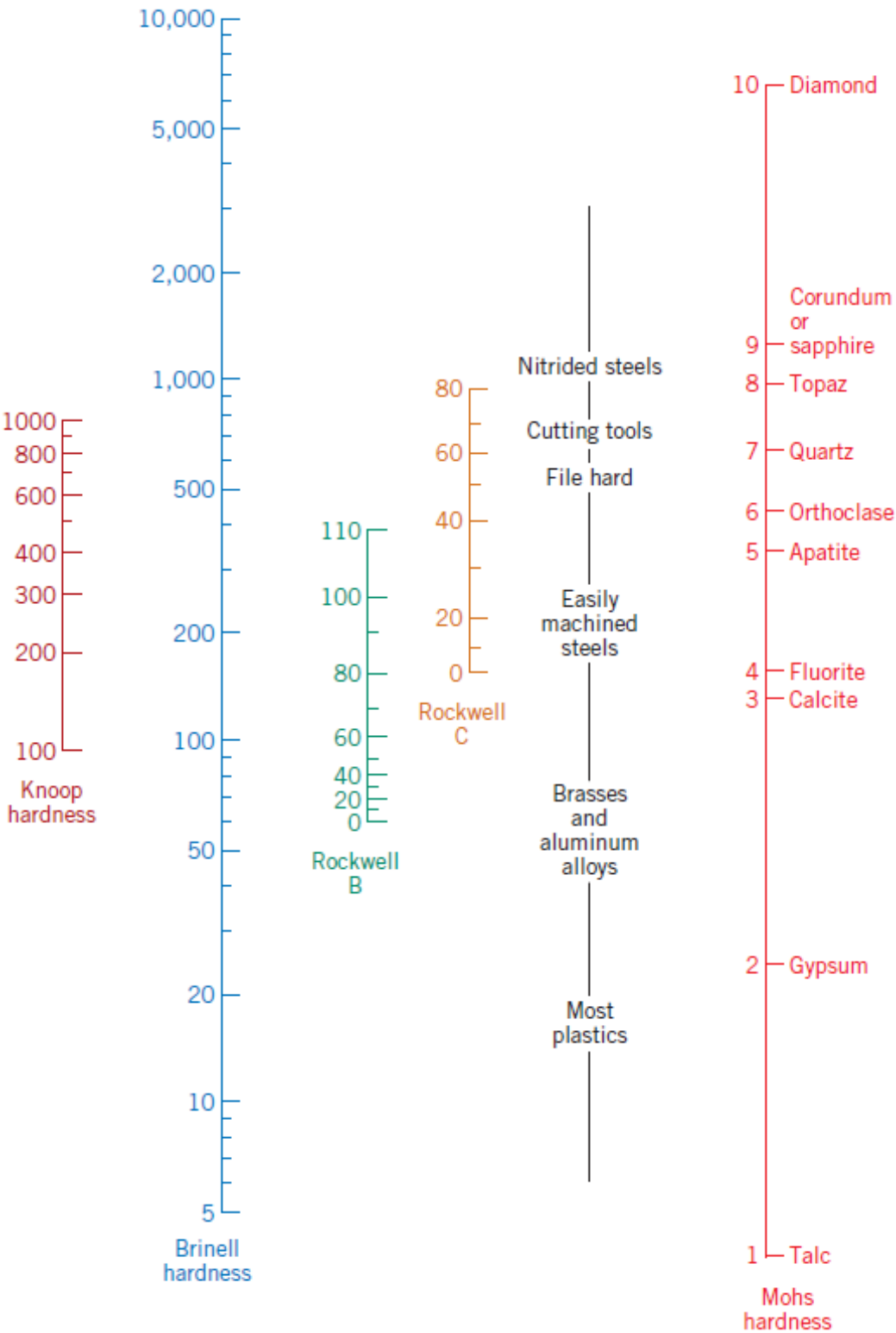
### **Background:**

Another mechanical property that may be important to consider is hardness, which is a measure of a material's resistance to localized plastic deformation (e.g., a small dent or a scratch) [1]. Hardness tests are performed more frequently than any other mechanical test for several reasons [1]:

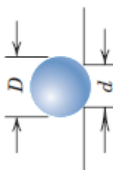
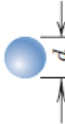


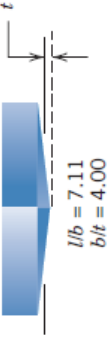
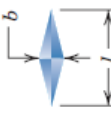
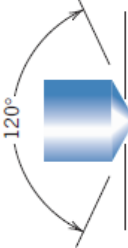

1. They are simple and inexpensive—ordinarily no special specimen need be prepared, and the testing apparatus is relatively inexpensive.
2. The test is nondestructive—the specimen is neither fractured nor excessively deformed; a small indentation is the only deformation.
3. Other mechanical properties often may be estimated from hardness data, such as tensile strength.

Early hardness tests were based on natural minerals with a scale constructed solely on the ability of one material to scratch another that was softer. A qualitative and somewhat arbitrary hardness indexing scheme was devised, termed the Mohs scale, which ranged from 1 on the soft end for talc to 10 for diamond (Figure 1). Quantitative hardness techniques have been developed over the years in which a small indenter is forced into the surface of a material to be tested, under controlled conditions of load and rate of application. The depth or size of the resulting indentation is measured, which in turn is related to a hardness number; the softer the material, the larger and deeper is the indentation, and the lower the hardness index number. Measured hardnesses are

only relative (rather than absolute), and care should be exercised when comparing values determined by different techniques (Figures 1 and 2).



**Figure 1.** Comparison of Several Hardness Scales [1].

Test	Shape of Indentation			Formula for Hardness Number <sup>a</sup>								
	Indenter	Side View	Top View									
Brinell	10-mm sphere of steel or tungsten carbide			$HB = \frac{2P}{\pi D[D - \sqrt{D^2 - d^2}]}$								
Vickers microhardness	Diamond pyramid			$HV = 1.854P/d_1^2$								
Knoop microhardness	Diamond pyramid			$HK = 14.2P/l^2$								
Rockwell and Superficial Rockwell	Diamond cone; $\frac{1}{16}, \frac{1}{8}, \frac{1}{4}, \frac{1}{2}$ in. diameter steel spheres			<table border="0"> <tr> <td>60 kg</td> <td rowspan="3">} Rockwell</td> </tr> <tr> <td>100 kg</td> </tr> <tr> <td>150 kg</td> </tr> <tr> <td>15 kg</td> <td rowspan="3">} Superficial Rockwell</td> </tr> <tr> <td>30 kg</td> </tr> <tr> <td>45 kg</td> </tr> </table>	60 kg	} Rockwell	100 kg	150 kg	15 kg	} Superficial Rockwell	30 kg	45 kg
60 kg	} Rockwell											
100 kg												
150 kg												
15 kg	} Superficial Rockwell											
30 kg												
45 kg												

<sup>a</sup> For the hardness formulas given,  $P$  (the applied load) is in kg, while  $D$ ,  $d$ ,  $d_1$ , and  $l$  are all in mm.

Source: Adapted from H. W. Hayden, W. G. Moffatt, and J. Wulff, *The Structure and Properties of Materials*, Vol. III, *Mechanical Behavior*. Copyright © 1965 by John Wiley & Sons, New York. Reprinted by permission of John Wiley & Sons, Inc.

Figure 2. Hardness-Testing Techniques [1].

### ***Rockwell Hardness Testing***

Rockwell hardness testing is the most widely used method for determining hardness, primarily because the Rockwell test is simple to perform and does not require highly skilled operators (Figures 2 and 3). By use of different loads (forces) and indenters, Rockwell hardness testing can determine the hardness of most metals and alloys, ranging from the softest bearing materials to the hardest steels. Readings can be taken in a matter of seconds with conventional manual operation and in even less time with automated setups. Optical measurements are not required; all readings are direct [2].

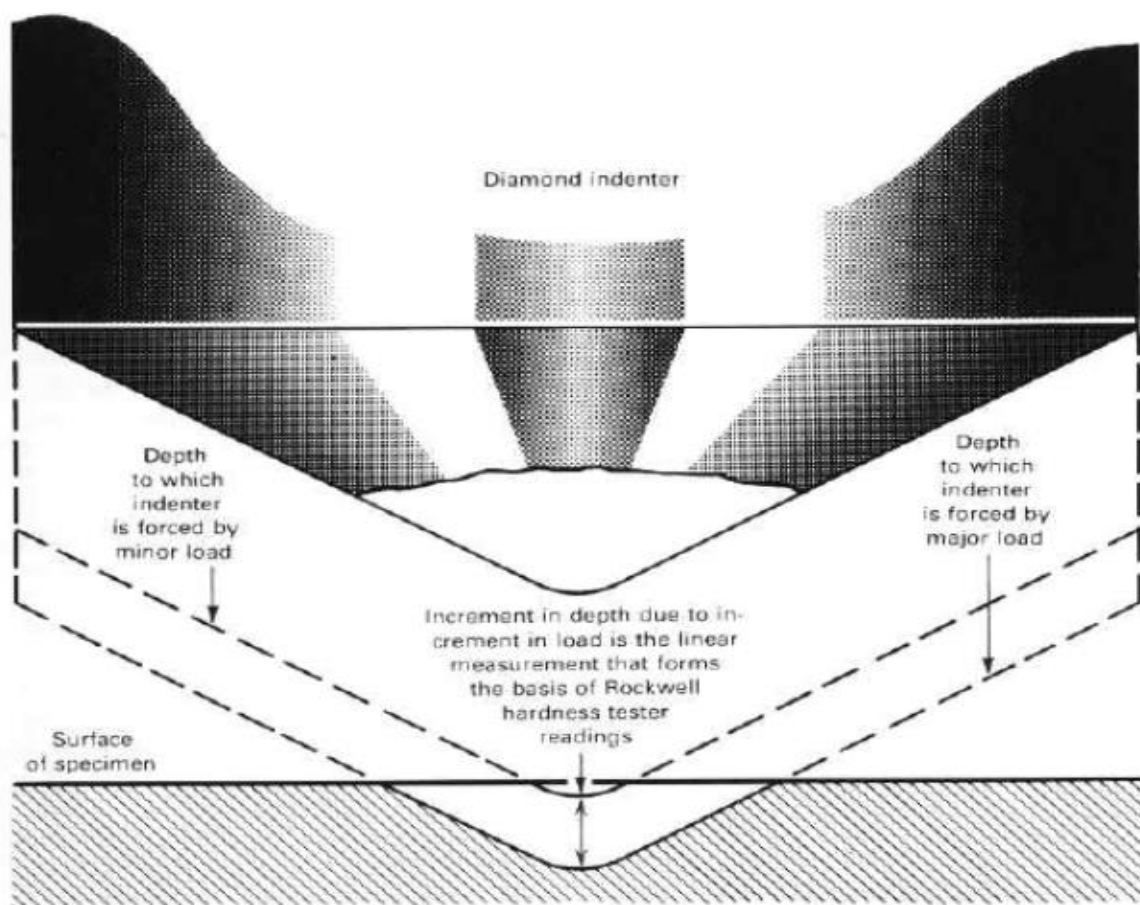


**Figure 3.** Principles of Rockwell Hardness Testing.

The Rockwell hardness test is a very useful and reproducible one provided that a number of simple precautions are observed. Most of the points filled below apply equally well to the other hardness tests:



- The indenter and anvil should be clean and well seated.
- The surface to be tested should be clean and dry, smooth, and free from oxide. A rough-ground surface is usually adequate for the Rockwell test.
- The surface should be flat and perpendicular to the indenter.
- Tests on cylindrical surfaces will give low readings, the error depending on the curvature, load, indenter, and hardness of the material. Theoretical and empirical corrections for this effect have been published.
- The thickness of the specimen should be such that a mark or bulge is not produced on the reverse side of the piece. It is recommended that the thickness be at least 10 times the depth of the indentation. The spacing between indentations should be three to five times the diameter of the indentation.
- The speed of application of the load should be standardized. This is done by adjusting the dashpot on the Rockwell tester. Variations in hardness can be appreciable in very soft materials unless the rate of load application is carefully controlled [3].

### ***Brinell Hardness Testing***

The Brinell hardness testing is a simple indentation test for determining the hardness of a wide variety of materials. The test consists of applying a constant load (force) usually between 500 and 3000 kg<sub>f</sub> for a specified time (10 to 30 s) using a 5- or 10-mm-diam hardened steel or tungsten carbide ball on the flat surface of a workpiece. The time period is required to ensure that plastic flow of the work metal has ceased. After removal the load, the resultant recovered round impression is measured in millimetres using a low-power microscope [2].

Hardness is determined by taking the mean diameter of the indentation (two readings at right angles to each other) and calculating the Brinell hardness number (BH) by dividing the applied load by the surface area of the indentation according to the following formula:

$$BH = \frac{F}{\frac{\pi}{2} D \cdot (D - \sqrt{D^2 - D_i^2})}$$

where;

BH= the Brinell hardness number,

F = the imposed load in kg,

D = the diameter of the spherical indenter in mm, and  
Di = diameter of the resulting indenter impression in mm.

### ***Vickers Hardness Testing***

The Vickers indenter (Figure 4) is a highly polished, pointed, square-based pyramidal diamond with face angles of 136°. With the Vickers indenter, the depth of indentation is about one seventh of the diagonal length.

When the mean diagonal of the indentation has been determined the Vickers hardness may be calculated from the formula but is more convenient to use conversion tables. The Vickers hardness that should be reported like 800 HV/10, which means a Vickers hardness of 800, was obtained using a 10 kg force. Several different loading settings give practically identical hardness numbers on uniform material, which is much better than the arbitrary changing of scale with the other hardness testing methods. The advantages of the Vickers hardness test are that extremely accurate readings can be taken, and just one type of indenter is used for all types of metals and surface treatments. Although thoroughly adaptable and very precise for testing the softest and hardest of materials, under varying loads, the Vickers machine is a floor standing unit that is more expensive than the Brinell or Rockwell machines [4].

The indenter employed in the Vickers test is a square-based pyramid whose opposite sides meet at the apex at an angle of 136°. The diamond is pressed into the surface of the material at loads ranging up to approximately 120 kilograms-force, and the size of the impression (usually no more than 0.5 mm) is measured with the aid of a calibrated microscope. The Vickers number (HV) is calculated using the following formula:

$$HV = \frac{2F \sin \frac{136^\circ}{2}}{d^2} \rightarrow HV = 1.854 \frac{F}{d^2}$$

where;

F= load in kgf,

d = arithmetic mean of the two diagonals, d<sub>1</sub> and d<sub>2</sub> in mm, and

HV = Vickers hardness.

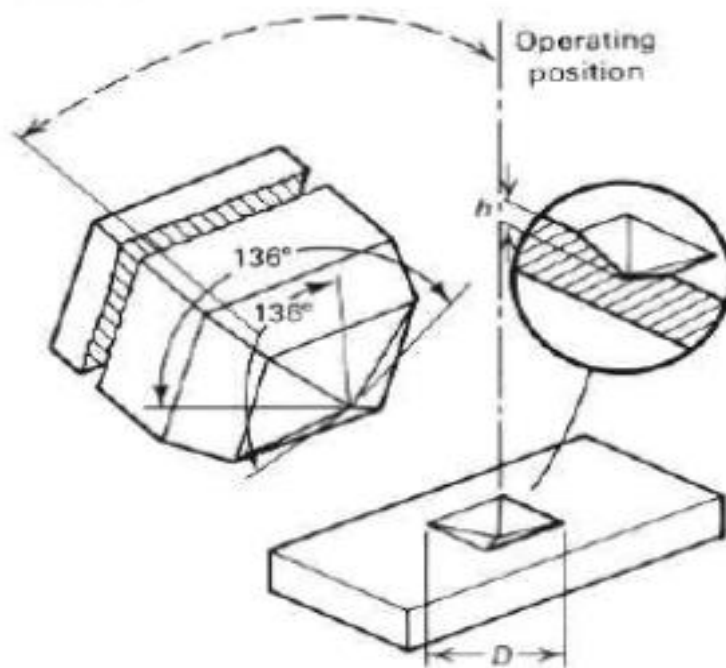


**Figure 4.** Diamond Pyramid Indenter Used for the Vickers Test and Resulting Indentation in the Work Piece.

### ***Knoop Hardness Testing***

The Knoop indenter (Figure 5) is a highly polished, rhombic-based pyramidal diamond that produces a diamond-shaped indentation with a ratio between long and short diagonals of about 7 to 1. The pyramid shape used has an included longitudinal angle of  $172^{\circ} 30'$  and an included transverse angle of  $130^{\circ} 0'$ . The depth of the indentation is about  $1/30^{\text{th}}$  of its length [2].

The diamond indenter employed in the Knoop test is in the shape of an elongated four-sided pyramid, with the angle between two of the opposite faces being approximately  $170^{\circ}$  and the angle between the other two being  $130^{\circ}$ . Pressed into the material under loads that are often less than one kilogram-force, the indenter leaves a four-sided impression about 0.01 to 0.1 mm in size. The length of the impression is approximately seven times the width, and the depth is  $1/30$  the length. Given such dimensions, the area of the impression under load can be calculated after measuring only the length of the longest side with the aid of a calibrated microscope. The final Knoop hardness (HK) is derived from the following formula [4]:

$$HK = \frac{P}{A} = \frac{P}{CL^2}$$

where;

P= the applied load, kgf,

A= the unrecovered projected area of the indentation in mm<sup>2</sup>,

L= the measured length of long diagonal of indentation in mm, and

C= 0.07028 = constant of indenter relating projected area of the indentation to the square of the length of the long diagonal.

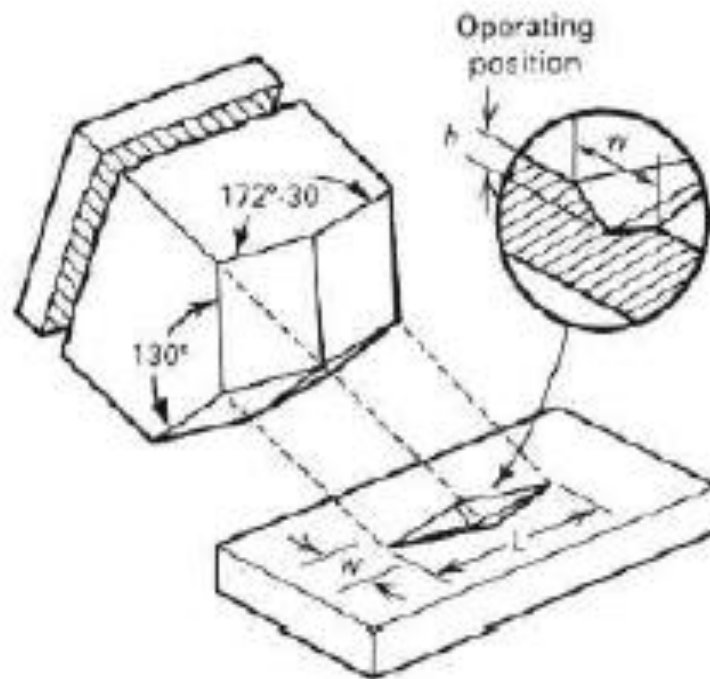


**Figure 5.** Pyramidal Knoop Indenter and Resulting Indentation in the Work Piece.

## References

1. W.D. Callister (2007) Materials Science and Engineering: An Introduction. 7<sup>th</sup> Edition. USA: John Wiley & Sons, Inc.
2. ASM Metal Handbook Volume 08 Mechanical Testing and Evaluation
3. <http://www.key-to-steel.com/Articles/Art140.htm>
4. <http://www.gordonengland.co.uk/hardness/vickers.htm>

## **Experiment # 3: Heat Treatment of Steels, Microstructure Analysis in Metallic Materials**

### **(a) Heat Treatment of Steels**

**Objective:** Investigation of conventional heat treatment procedures used to tailor the properties of steels. Effects of heat treatment and different cooling conditions on microstructure and hardness.

**Materials:** AISI 4140 alloy steel, heat treatment oil (Petrofer isorapid 277hm)

**Equipment:** Box furnace, oil and water baths.

#### **Background:**

Metals and alloys for many structural and mechanical applications need to be hard, strong and tough. These required properties are dependent mainly on composition, and microstructure of the steel. On the microstructural level, the size and distribution of the phases and grains controls the mechanical properties. A metal having a fine-grained microstructure yields higher hardness, strength and toughness values when compared to one having a coarse-grained microstructure. But the mechanical properties depend strongly on the phases present than the grains. Heat treatment is a combination of heating and cooling operations timed and applied to a metal or alloy in the solid state in a way that will produce desired microstructure and properties. All basic heat-treating processes for steels involve the transformation or decomposition of austenite.

#### **Heat treatment types [3]:**

##### **1. Annealing**

- Normalization
- Softening
- Spheroidizing
- Stress relieving
- Coarse grain annealing
- Diffusion annealing

##### **2. Hardening**

**3. Reclamation** (Reclamation is a process that gives great strength, high yield strength, high ductility and also plasticity to workpieces and building elements.

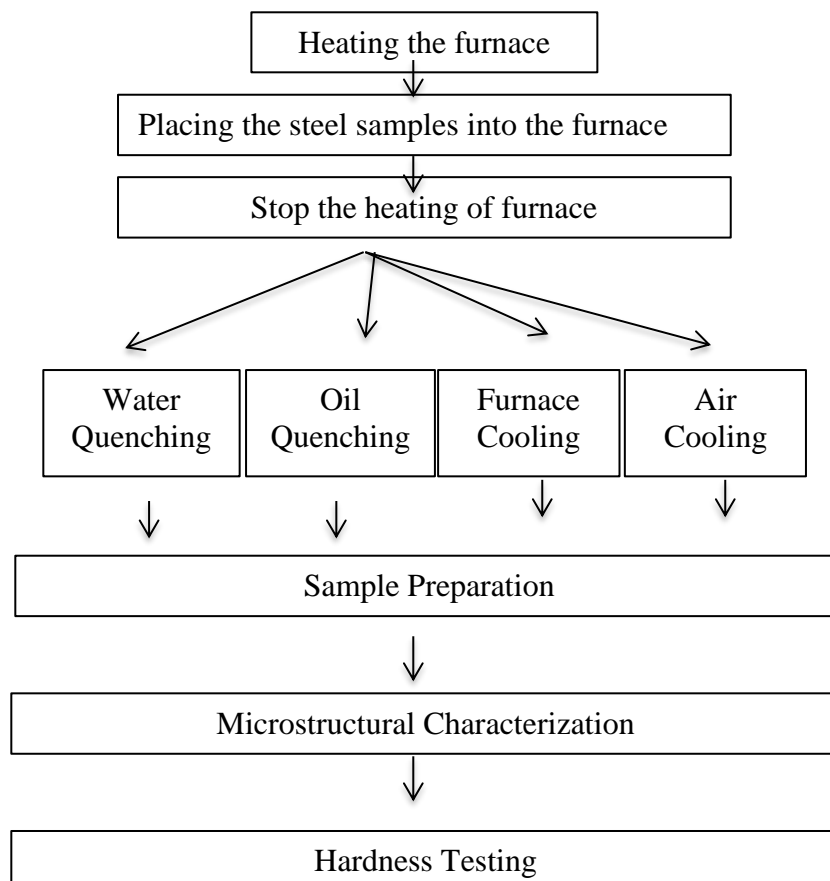
##### **4. Surface hardening**

- Carburation
- Nitriding
- Flame surface hardening
- Induction hardening

### Possible Heat Treatment Goals/Aims [3];

1. To improve the workability (softening, grain blooming)
2. To increase or decrease strength (hardening, normalization, softening temper)
3. To remove adverse effects of cold shaping (recrystallization)
4. To remove micro segregation (diffusion)
5. To adjust grain size (normalization, recrystallization, coarse grain)
6. To reduce internal stresses (stress relief)
7. To adjust microstructure (normalization, softening, hardening)

### Experimental Procedure



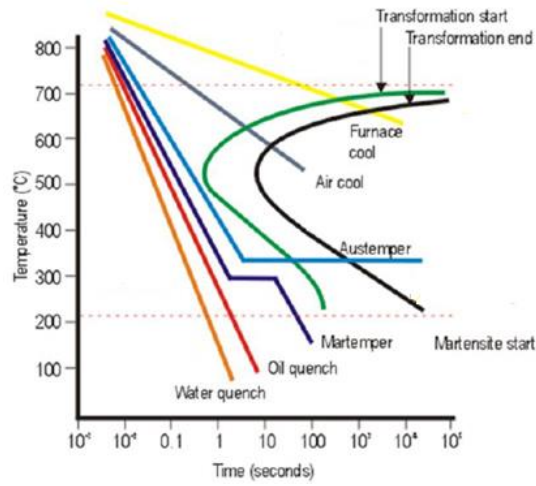


**Figure 1.** Various cooling curves on the IT diagram [3].

### Continuous Cooling Transformation (CCT) diagram [3]

Definition: Stability of phases during continuous cooling of austenite

There are two types of CCT diagrams:

- I. Plot of (for each type of transformation) transformation start, specific fraction of transformation and transformation finish temperature against transformation time on each cooling curve.
- II. Plot of (for each type of transformation) transformation start, specific fraction of transformation and transformation finish temperature against cooling rate or bar diameter for each type of cooling medium.

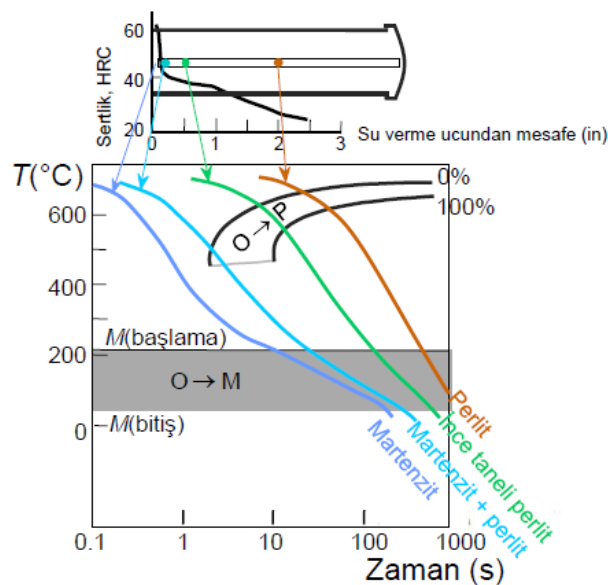


**Figure 2.** CCT Diagram.

### Isothermal Transformation (IT) or Time-Temperature Transformation (TTT) Diagrams [3]

- I. Indicates the amount of transformation at a constant temperature.
- II. Samples are austenitised and then cooled rapidly to a lower temperature and held at that temperature whilst the amount of transformation is measured, for example by dilatometry.
- III. Obviously a large number of experiments are required to build up a complete TTT diagram.

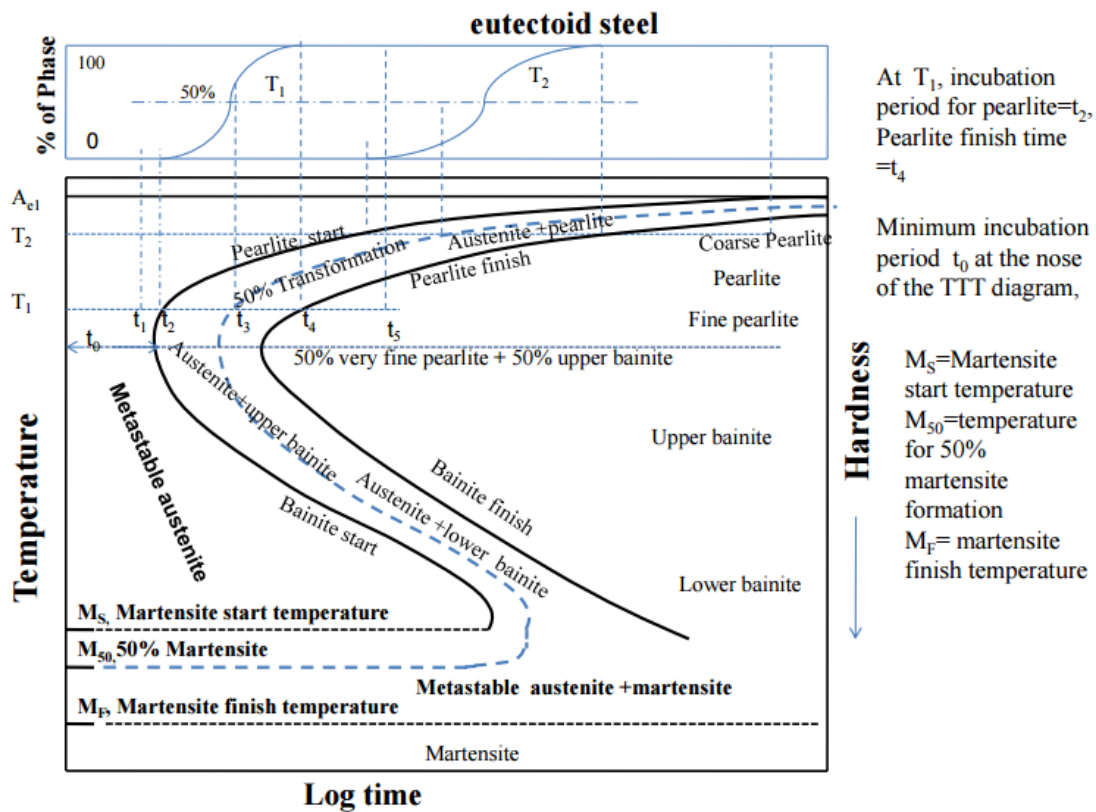


Figure 3. TTT diagram.

The microstructure of any heat-treated metal is deduced using Continuous Cooling Transformation (CCT) diagrams which is related to the Time-Temperature-Transformation (TTT) or Isothermal Transformation (IT) of the selected metal sample. The CCT diagram for 4140 steel is shown in Figure 4.



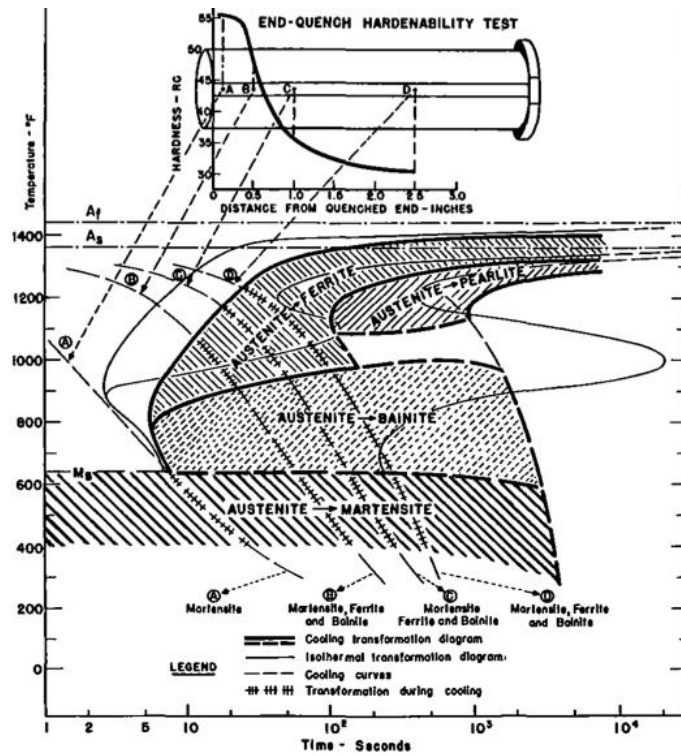


Figure 4. CCT diagram of 4140 steel [1].

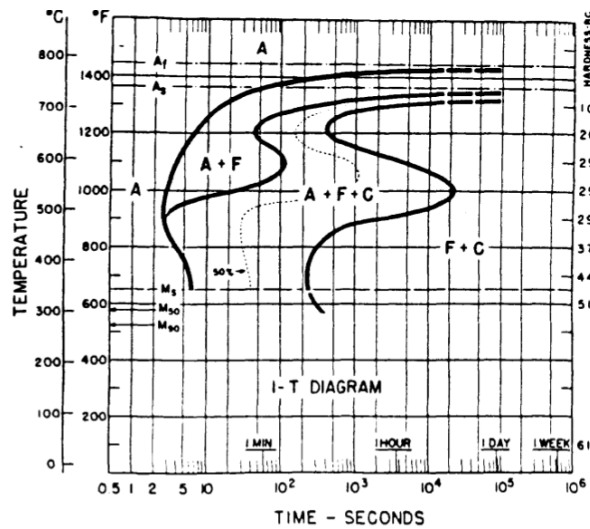


Figure 5. TTT diagram of 4140 steel [2].

## REFERENCES

1. Voort, G.F.V., Atlas of Time-Temperature Diagrams for Irons and Steels
2. ASM, Atlas of isothermal transformation and cooling transformations diagrams.
3. ASM 2012, F.C.Campbell, Phase Diagrams Understanding The Basics.

## **(b) Microstructure Analysis in Metallic Materials**

**Objective:** The purpose of this laboratory is to acquaint students with the manner in which metallurgical specimens are prepared for metallographic study, to correlate the relationship between cooling rate and microstructure development.

**Materials:** A set of polished and etched identified and unidentified metal specimens.

**Equipment:** Metallographic preparation facilities and optical microscopes.

### **Background:**

#### **1. Introduction**

A properly prepared metallographic sample can be aesthetically pleasing as well as revealing from a scientific point of view. The purpose of this practical is to understand how to prepare and interpret metallographic samples systematically. The process is illustrated below.

- Gather information about chemical composition, heat treatment, processing and phase diagram.
- Cut out representative samples, noting plane of section relative to prominent features (e.g. long direction of rod).
- Mount, grind and polish the sample.
- Examine unetched sample.
- Etch lightly and examine again.
- Etch further if necessary.
- Compare obtained microstructure with the one predicted referring to the equilibrium phase diagram.

You are provided with these samples: hypo-eutectoid steel, eutectoid steel, hyper-eutectoid steel, martensitic steel, pearlitic-ferritic grey cast iron, lamellar (flake) graphite grey cast iron, Spheroidal (nodular) graphite cast iron, white cast iron, brass (alloy of copper and zinc).

#### ***1.1 Sample Mounting***

Small samples can be difficult to hold safely during grinding and polishing operations, and their shape may not be suitable for observation on a flat surface. They are therefore mounted inside a polymer block. This can be done cold using two components which are liquid to start with but which set solid shortly after mixing. Cold mounting requires very simple equipment consisting of a cylindrical ring which serves as a mould and a flat piece of glass which serves as the base of the mould. The sample is placed on the glass within the cylinder and the mixture poured in and allowed to set. Cold mounting takes about 40 minutes to complete.

In hot-mounting the sample is surrounded by an organic polymeric powder which melts under the influence of heat (about 200°C). Pressure is also applied by a piston, ensuring a high quality mould free of porosity and with intimate contact between the sample and the polymer. This is not the case with cold mounting where the lack of proper contact and the presence of porosity can cause problems such as the entrapment and seepage of etchant during the final stages of preparation. Consequently, hot-mounting should be the preferred way of encapsulating specimens assuming that time and resources permit, and assuming that the heat involved in the process does not influence the sample.

## ***1.2 Grinding and Polishing***

Grinding is done using rotating discs covered with silicon carbide paper and water. There are a number of grades of paper, with 180, 240, 400, 1200 grains of silicon carbide per square inch. 180 grade therefore represents the coarsest particles and this is the grade to begin the grinding operation. Always use light pressure applied at the center of the sample. Continue grinding until all the blemishes have been removed, the sample surface is flat, and all the scratches are in a single orientation. Wash the sample in water and move to the next grade, orienting the scratches from the previous grade normal to the rotation direction. This makes it easy to see when the coarser scratches have all been removed. After the final grinding operation on 1200 paper, wash the sample in water followed by alcohol and dry it before moving to the polishers.

The polishers consist of rotating discs covered with soft cloth impregnated with diamond particles (6 and 1 micron size) and an oily lubricant. Begin with the 6 micron grade and continue polishing until the grinding scratches have been removed. *It is of vital importance that the sample is thoroughly cleaned using soapy water, followed by alcohol, and dried before moving onto the final 1 micron stage.* Any contamination of the 1 micron polishing disc will make it impossible to achieve a satisfactory polish.

### ***1.3 Etching***

The purpose of etching is two-fold. Grinding and polishing operations produce a highly deformed, thin layer on the surface which is removed chemically during etching. Secondly, the etchant attacks the surface with preference for those sites with the highest energy, leading to surface relief which allows different crystal orientations, grain boundaries, precipitates, phases and defects to be distinguished in reflected light microscopy.

<b>2% Nital</b>	<b>Ferric Chloride</b>	<b>Sodium Hydroxide</b>
Steel	Stainless steel	Aluminium & alloys
	Copper & alloys	Zinc & alloys
-	-	Magnesium & alloys

A polished sample is etched using a cotton tip dipped in the etchant. Etching should always be done in stages, beginning with light attack, an examination in the microscope and further etching only if required. If you overetch a sample on the first go then the polishing procedure will have to be repeated.

### ***1.4 Metallographic Imaging Modes***

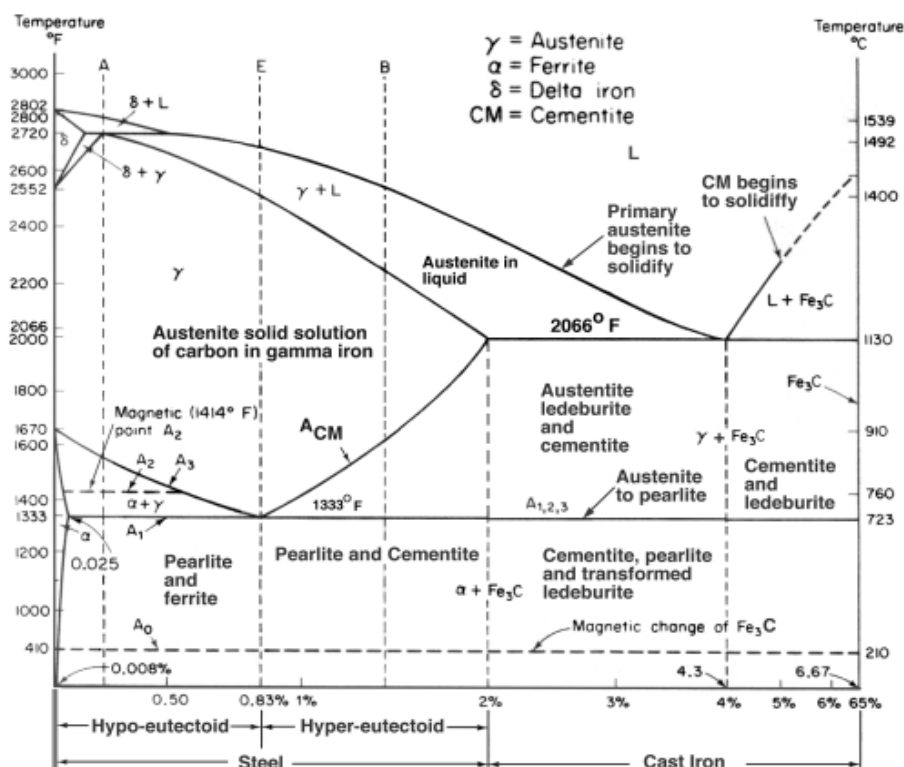
The reflected light microscope is the most commonly used tool for the study of the microstructure of metals. It has long been recognized that the microstructure of metals and alloys has a profound influence on many of the properties of the metal or alloy. Mechanical properties (strength, toughness, ductility, etc.) are influenced much more than physical properties (many are insensitive to microstructure). The structure of metals and alloys can be viewed at a wide range of levels - macrostructure, microstructure, and ultra-microstructure.

In the study of microstructure, the metallographer determines what phases or constituents are present, their relative amounts, and their size, spacing, and arrangement. The microstructure is established based upon the chemical composition of the alloy and the processing steps.

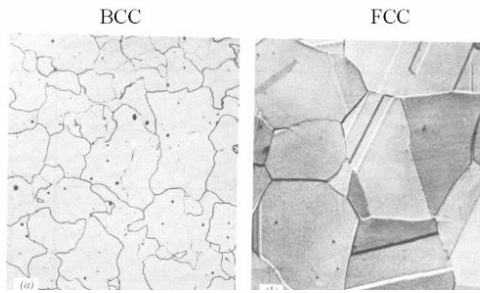
## **2. Microstructures**

### ***2.1 Steel***

**Steel** is an alloy consisting mostly of iron, with a carbon content between 0.2 and 1.7 or 2.04% by weight (C:1000–10,8.67Fe), depending on grade. Carbon is the most cost-effective alloying material for iron, but various other alloying elements are used such as manganese, chromium, vanadium, and tungsten. Carbon and other elements act as a hardening agent, preventing dislocations in the iron atom crystal lattice from sliding past one another. Varying the amount of alloying elements and form of their presence in the steel (solute elements, precipitated phase) controls qualities such as the hardness, ductility and tensile strength of the resulting steel. Steel with increased carbon content can be made harder and stronger than iron, but is also more brittle. The maximum solubility of carbon in iron (in austenite region) is 2.14% by weight, occurring at 1149 °C; higher concentrations of carbon or lower temperatures will produce cementite. Alloys with higher carbon content than this are known as cast iron because of their lower melting point. Steel is also to be distinguished from wrought iron containing only a very small amount of other elements, but containing 1–3% by weight of slag in the form of particles elongated in one direction, giving the iron a characteristic grain. It is more rust-resistant than steel and welds more easily. It is common today to talk about 'the iron and steel industry' as if it were a single entity, but historically they were separate products.



### Microstructure of Ferrite and Austenite



Microstructure of hyper eutectoid steel

## 2.2 Cast Irons

Cast irons with a composition equivalent to about 4.3% C solidify as a eutectic. Because cast irons are not simple binary Fe-C alloys, it is usual practice to calculate the carbon equivalent (CE) value which is the total carbon content plus one-third the sum of the silicon and phosphorus contents. If the CE is  $> 4.3$ , it is hypereutectic; if it is  $< 4.3$ , it is hypoeutectic.

In the Fe-C system, the carbon may exist as either cementite, Fe<sub>3</sub>C, or as graphite. So the eutectic reaction is either liquid transforming to austenite and cementite at about 1130°C or liquid transforming to austenite and graphite at about 1135°C. Addition of elements such as silicon promote graphite formation. Slow cooling rates promote graphite formation, while higher rates promote cementite. The eutectic grows in a cellular manner with the cell size varying with cooling rate which influences mechanical properties.

### 2.2.1 Gray Iron

Figure 1 shows interdendritic flake graphite in a hypoeutectic alloy where proeutectic austenite forms before the eutectic reaction. This type of graphite has been given many names. In the US it is referred to as Type D (ASTM A247) or as undercooled graphite. It was thought that the fine size of the graphite might be useful, but it is not technically useful as it always freezes last into a weak interdendritic network.

Figure 2 shows more regularly-shaped graphite flakes in an alloy of higher carbon content, although still hypoeutectic. While flake lengths in Figure 1 are roughly 15-30µm, flake lengths in Figure 2 are in the 60-120µm range. Figure 3 shows somewhat coarser flakes (250-500µm length range) in a higher carbon content cast iron.

Other graphite forms are also observed. For example, Figure 4 shows disheveled graphite flakes in a casting. Note that a few nodules are present. This appears to be a mix of B- and D-type flakes. Figure 5 shows a hypereutectic gray iron where very coarse flakes form before the eutectic which is very fine. This is similar to C-type graphite.

### 2.2.2 Nodular Iron

The addition of magnesium ('inoculation') desulfurizes the iron and causes the graphite to grow as nodules rather than flakes. Moreover, mechanical properties are greatly improved over gray iron; hence, nodular iron is widely known as 'ductile iron'.

Nodule size and shape perfection can vary depending upon composition and cooling rate. Figure 6 shows fine nodules, about 15-30 $\mu\text{m}$  in diameter, while Figure 7 shows coarser nodules (about 30-60 $\mu\text{m}$  diameter) in two ductile iron casts. Note that the number of nodules per unit area is much different, about 350 per  $\text{mm}^2$  vs. 125 per  $\text{mm}^2$ , respectively.

### 2.2.3 Compacted Graphite

Compacted graphite is a more recent development made in an effort to improve the mechanical properties of flake gray iron. Figure 8 shows an example where the longest flakes are in the 60-120 $\mu\text{m}$  length range. Compare these flakes to those shown in Figures 2 and 3.



Figure 1

Figure 2

Figure 3

Figure 4

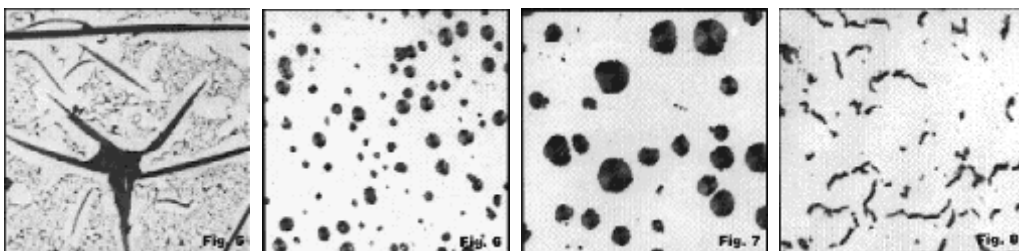


Figure 5

Figure 6

Figure 7

Figure 8

## **Experiment # 4: OES Spectrometer**

**Objective:** Understanding the quantitative analysis of various metallic materials

**Materials:** Steel, Al, Cu, Mg and Ti samples

**Equipment:** Optical Emission Spectrometer

### **Background:**

There are several techniques for quantitative analysis used for metals characterization. Most common techniques are spark optical emission spectroscopy (spark OES, which is the technique used in this experiment), inductively coupled plasma spectroscopy (ICP-OES), x-ray fluorescence spectroscopy (XRF) and combustion methods.

ICP-OES is a technique to analyze the concentration of metallic elements in solid/liquid samples. Like spark OES, ICP-OES uses the optical emission principles of excited atoms for the determination of their elemental concentrations. The difference is in ICP-OES, solid samples are dissolved in an appropriate solvent (typically acid) to produce a solution for analysis. The intensities of the characteristic wavelengths are measured then compared to intensities for known standards for quantitative results. All metallic elements can be detected. The minimum detection limits are typically parts per million to parts per billion for the dissolved samples.

XRF is a technique that can be used for direct analysis of solid metals, thin metal films, petroleum products, cement, coal, etc. The energy of x-rays and their intensities are measured. Elements from Be to U can be detected. The minimum detection limits are typically in the parts per million range. Because the characteristic x-ray intensity will vary with the thickness of films on a substrate of different material, thin film thickness can also be measured by XRF. The samples may be solids, liquids or powders. Samples often require little to no preparation prior to analysis.

In combustion methods, high temperature combustion is used to determine C and S content in a variety of metals. Lower detection limits for carbon range from 0.1 to 10 parts per million with upper detection limits of 2.5-3.5 %. Lower detection limits for sulfur range from 0.1 to 50 parts per million with upper detection limits of 0.2-2.5 %. One gram or less of a solid, chips, or powder



sample is typically required. Samples should not be contaminated with sulfur or carbon prior to analysis.

Optical Emission Spectroscopy (OES), is a widely used analytical characterization technique for determining the elemental compositions of metals.

Types of samples, which can be characterized using OES, include samples from the melt in primary and secondary metal production, and parts from metal processing industries, tubes, bolts, rods, wires, plates, etc. Metal producing industries like foundries, steel, copper, aluminum plants, and automotive, aviation, home appliance industries, inspection companies, research laboratories and metal recyclers use OES for process and quality control.

The part of the electromagnetic spectrum which is used by OES includes the visible spectrum and part of the ultraviolet spectrum (thus called UV-VIS spectrometry). In terms of wavelength from 130 nm up to 800 nm as seen of Figure 1.

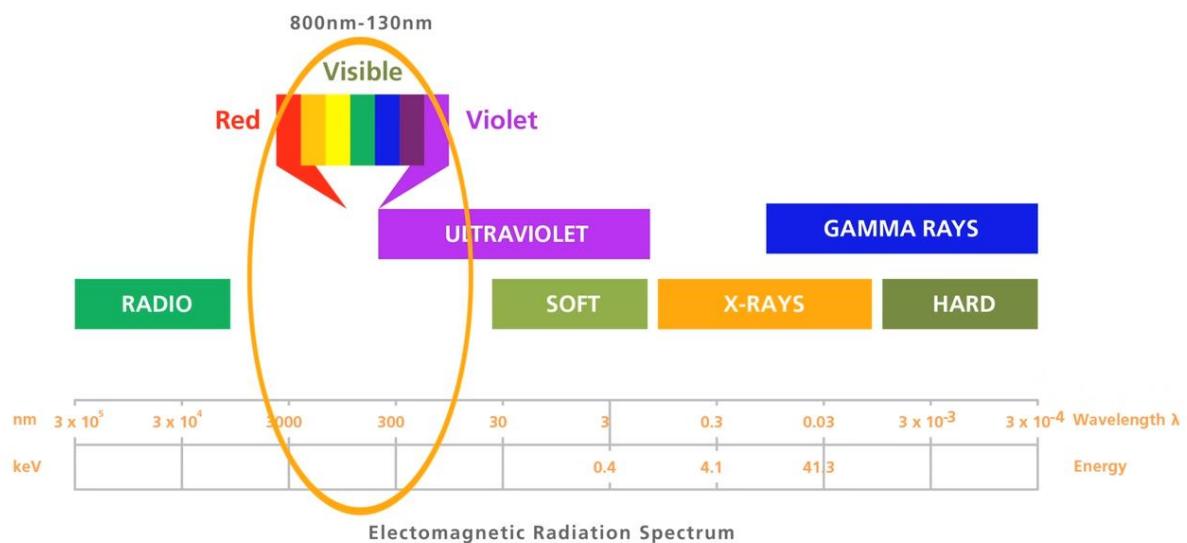


**Figure 1.** Part of electromagnetic spectrum used by OES.

The quality and quantity of elements that can be determined by OES depends on the material and the type of analyzer used.

The working of an OES system is shown on Figure 2. OES involves applying electrical energy in the form of spark generated between an electrode and a metal sample, vaporizing atoms and bringing them to a high energy state within a so-called “discharge plasma”.

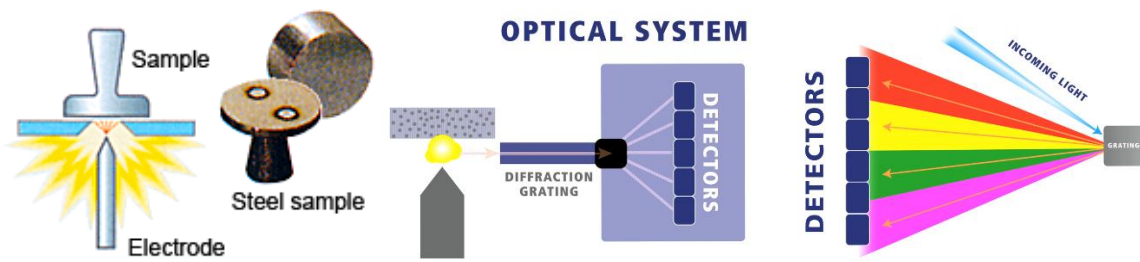


**Figure 2.** How OES works.

Excited atoms in the discharge plasma create a unique emission spectrum specific to each element and a single element generates numerous characteristic emission spectral lines. The light generated by the discharge is a collection of the spectral lines generated by the elements in the sample. This light is split by a diffraction grating to extract the emission spectrum for the target elements. The intensity of each emission spectrum depends on the quantity of the element in the sample. Detectors (photomultiplier tubes) measure the presence or absence of the spectrum extracted for each element and the intensity of the spectrum to perform qualitative and quantitative analysis of the elements.

### Experimental Procedure

1. Prepare the spectrometer for the steel sample, place proper electrode and optical interface.
2. Take a measurement 3-5 times from different areas of sample surface.
3. Take a note of metallic elements contained in the sample.
4. Calculate mean quantity and standard deviation for each element.
5. Repeat the same steps for Al, Cu, Mg and Ti samples.

### References

1. Skoug, D. A., Holler, F. J. and Crouch, S. R. (2007). Principles of Instrumental Analysis, 6<sup>th</sup> ed. Thompson Brooks/Cole, Canada.
2. <http://www.mee-inc.com/hamm/quantitative-chemical-analysis/>
3. <http://www.the-experts.com/optical-emission-spectroscopy-oes-explained>
4. <http://www.shimadzu.com/an/elemental/oes/oes.html>
5. <https://www.bruker.com/products/x-ray-diffraction-and-elemental-analysis/optical-emission-spectrometry.html>

## **Experiment # 5: Polymer Processing, Thermal Characterization of Polymeric Materials**

### **(a) Polymer Processing**

**Objective:** Processing of polymers through extrusion, followed by the strand pelletizing process.

**Materials:** Polypropylene (PP)

**Equipment:** Twin-screw extruder

### **Background:**

#### **1. Introduction**

By definition, extrusion stands for a continuous process of producing a semi-finished part. During extrusion, a polymer melt is pumped through a die and formed into a shape. This shape can be a profile, plate, film, tube, or have any other shape formed from its cross section. During extrusion, the melt can be mixed, densified, plasticized, homogenized, degassed, or chemically altered (reactive extrusion). A subsequent treatment of the semi-finished material before solidification e. g. by pressured air or calendaring is also possible. Since the polymer is completely melted during extrusion and brought into a new form, the extrusion process is a primary shaping process. In this experiment a small twin screw extruder is used to produce polypropylene films. Some film properties are investigated as function of selected extrusion parameters.

#### **2. Extrusion Equipment**

An extrusion system consists not only of a plasticizing extruder, but also of additional auxiliary parts and add-ons, whose design and function are more closely described in the following text. Requirements for all extrusion systems are: i) homogeneous transport of the material, ii) production of a thermally and mechanically homogenous melt, iii) processing of the polymer while avoiding thermal, chemical, or mechanical degradation and iv) providing an economic process with profitable operation. Common machines are single and twin-screw extruders. Generally, single screw extruders are used for pumping high mass throughputs at high pressures

needed for large parts such as pipes, plates, or profiles. Twin-screw extruders are preferably employed for mixing and compounding, as well as polymerization reactors. Parts of an extruder are hopper, barrel, screw, heating/cooling, and drive/gear.

## 2.1. Single screw extruder

The plasticizing single screw extruder is the most common equipment in the polymer industry. It can be part of an injection molding unit and is found in numerous other extrusion processes, including blow molding, film blowing and wire coating. Its function is to produce a homogeneous melt from the supplied plastics pellets and to press the melt through the shaping die. The tasks of a plasticizing extruder are to i) transport the solid pellets or powder from the hopper to the screw channel, ii) compact the pellets and move them down the channel, iii) melt the pellets, iv) mix the polymer into a homogeneous melt and v) pump the melt through a die. Thus an extrusion system consists of the components shown in Figure 1.

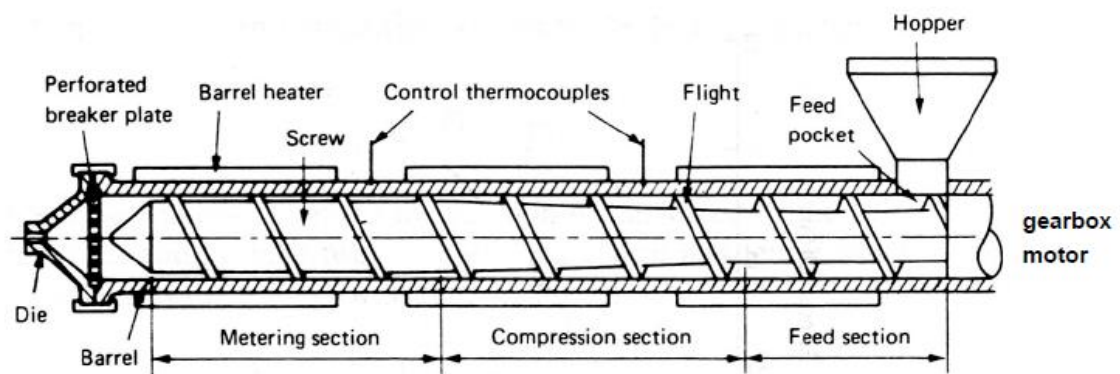


**Figure 1:** Schematic of a plasticating single screw extruder [4].

The screw is the central element of extrusion and serves many functions such as transporting the solid feedstock, compressing, melting, homogenizing, and metering the polymer to finally generate sufficient pressure to pump the melt through the die. Most commonly are three-zone screws (Figure 2-4), since they can be used universally for most thermoplastics. The size of an extruder is defined by the internal diameter  $D$  (see Fig. 2), which is normally in the range of 20 to 150 mm. The  $L/D$  ratio ranges from 5 to 34. Shorter machines ( $L/D < 20$ ) are generally used for processing elastomers, longer machines for thermoplastics. For special purposes grooved barrels are used which improve transport and compression. Barrel temperatures are controlled by electrical heaters and fans. Temperatures and pressure at certain barrel positions are monitored by thermocouples or pressure gauges, respectively. By using several temperature zones a

temperature profile can be easily realized. The hopper (see Fig. 1) has the function to supply the pellets or powder to the extrusion screw. In larger systems the hopper is often equipped with an additional agitating or conveyer system. A dryer can be also attached for moisture-sensitive materials. For the coloring or mixing of several components gravimetrically or volumetrically dosage systems are available.

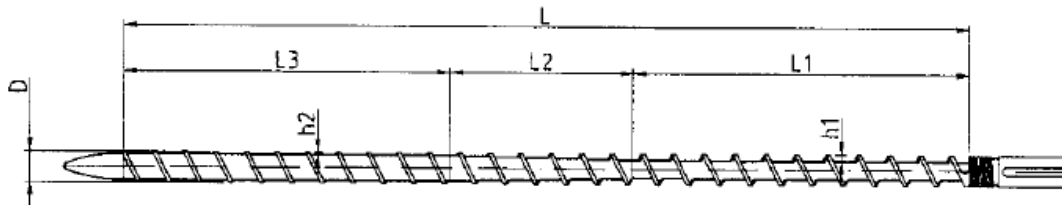


**Figure 2:** Three-zone extrusion screw. D: diameter; L: total length; L1: (length) solid conveying zone/feed section/compaction; L2: Melting/compression/transition zone; L3: metering/pumping zone; h1 and h2: channel depth h (or H). An extruder is characterized by its L/D ratio, e. g. 25 (D= 20 mm, L= 0.5 m).

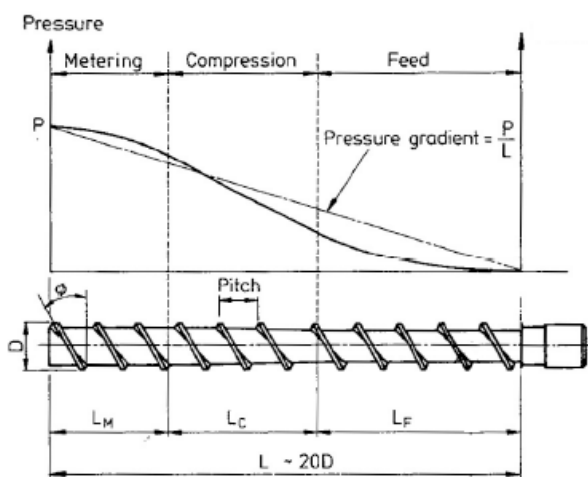


**Figure 3:** Typical zones of a single extruder screw and the corresponding pressure build-up. [4]

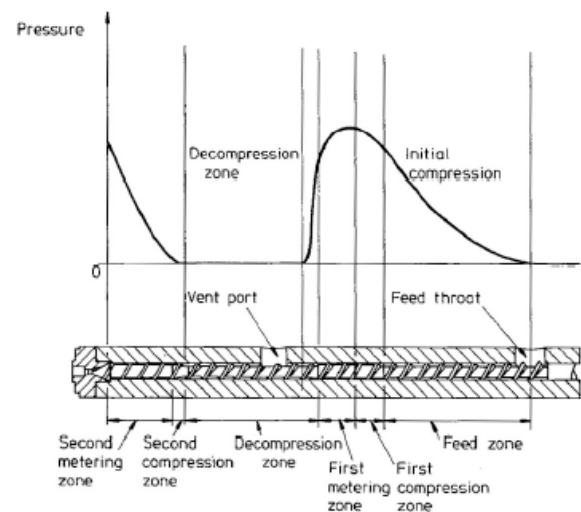


**Figure 4:** Typical zones of a single extruder screw with vent port and the corresponding pressure build-up. [4]

For better temperature control in large extruders, screws can be also heated from inside. The task of the solids conveying zone in the feed section is to move the polymer pellets/powder from the hopper to the screw channel. The most common feed from the hopper is by gravity (flood feed), the screw continuously extracts the resin it can handle from the hopper. Once the material is in the screw channel, it is compacted and transported down the channel. Compacting and moving can only be accomplished by friction at the screw surface. To maintain a high coefficient of

friction between the barrel and polymer, the feed section of the barrel must be cooled by water. The frictional forces result in a pressure rise in the feed section, this pressure compresses the solid bed which continues to travel down the channel as it melts in the compression or melting zone. This effect is amplified by a decreasing channel depth compared to the conveying zone. The metering zone is the most important section in melt extruders and the pressure for sufficient pumping and final melt temperatures are generated here. In this section the screw depth is again constant but much less than the feeding zone. In the metering zone the melt is homogenized so as to supply a constant rate, material of uniform temperature and pressure to the die. The zone is the most straight-forward to analyze since it involves a viscous melt flowing along a uniform channel. The pressure build-up which occurs along a screw is shown in Figure 3 and Figure 4. Some extruders also have a venting zone to remove volatile components such as water vapor or other low molecular weight impurities. As shown in Figure 4, in the first part of the screw the granules are taken in and melted, compressed and homogenized in the usual way. The melt pressure is then reduced to atmospheric pressure in the decompression zone. This allows volatiles to escape from the melt through a special port (vent port) in the barrel. The melt is then conveyed along the barrel to a second compression zone which prevents air pockets from being trapped. The venting port works because at a typical extrusion temperature of 250°C the water in the melt exists as a vapor at a pressure of about 4 MPa (40 bar). At this pressure it will easily pass out of the melt end through the vent. Since the atmospheric pressure is about 0.1 MPa the application of a vacuum will have little effect on the removal of moisture. Figure 5 shows a more detailed view of a screw element. Here  $D$  denotes the standard diameter of the barrel minus twice the screw clearance which is around 100  $\mu\text{m}$  for  $D < 30$  mm;  $\Phi$  the helix angle with a typical value for a square pitch screw of 17.65°;  $H$  (also denoted as  $h$ ) is the channel depth in the metering section which is in the range of  $0.05\text{-}0.07 \cdot D$  for  $D < 30$  mm;  $C$  is the pitch of the screw;  $e$  the width of the screw flights;  $W$  the width of the melt channel. Knowing these parameters the pumping characteristics of an extruder can be represented with sets of die and screw characteristic curves.

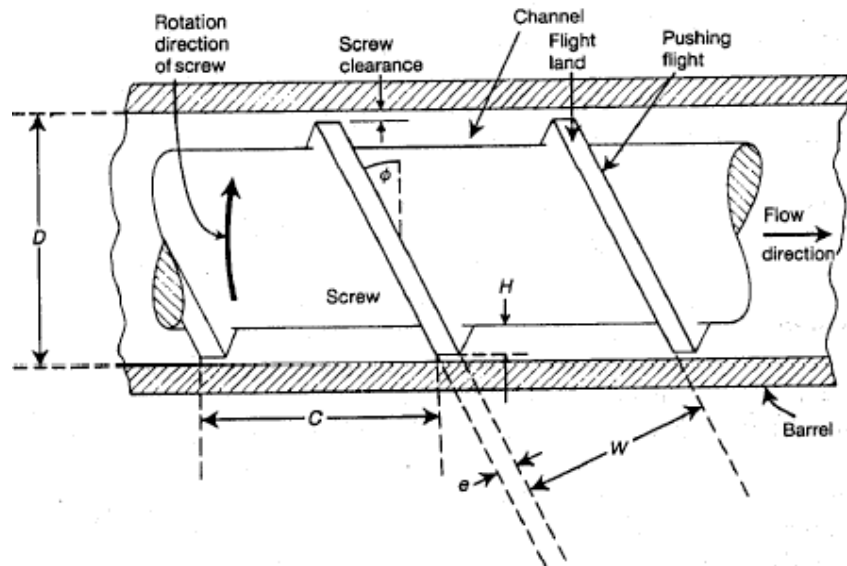


**Figure 5.** Screw section

First, in Figure 6, the die characteristic curves are labeled die 1, die 2, die 3 and die 4 in ascending order of die restriction. Here, die 1 represents a low resistance die such as for a thick plate, and die 4 represents a restrictive die, such as is used for films. The difference screw characteristic curves represent different screw rotational speeds  $N$ . In a screw characteristic curve the point of maximum throughput and no pressure build-up is called point of open discharge. This occurs when there is no die. The point of maximum pressure build-up and no throughput is called the point of closed discharge. This occurs when the extruder is plugged. Shown also in Figure 6, the feasibility line represents the throughput required to have an economically feasible system. For an ideal Newtonian fluid in the metering zone linear relationships are obtained as shown in Figure 7.

Here two interesting situations are to consider. One is the case of free discharge where there is no pressure build-up ( $\Delta p = 0$ ) at the end of the extruder and the ordinate is intersected at maximum throughput. The other case is where the pressure at the end of the extruder is large enough to stop the output and ignoring leakage flow. These are the limits of the screw characteristic. It is interesting to note, that when a die is coupled to the extruder, the requirements are conflicting. The extruder has a high output if the pressure at its outlet is low. However, the outlet from the extruder is the inlet of the die and the output of latter increases with inlet pressure. The intersection of both characteristic curves is the operating point of the extruder. Figure 7 also shows the influence of channel depth for the metering zone of a conventional, smooth barrel single screw extruder on the screw characteristic curves. A restrictive extrusion would clearly

work best with a shallow channel screw, and a less restrictive die would render the highest productivity with a deep channel screw.

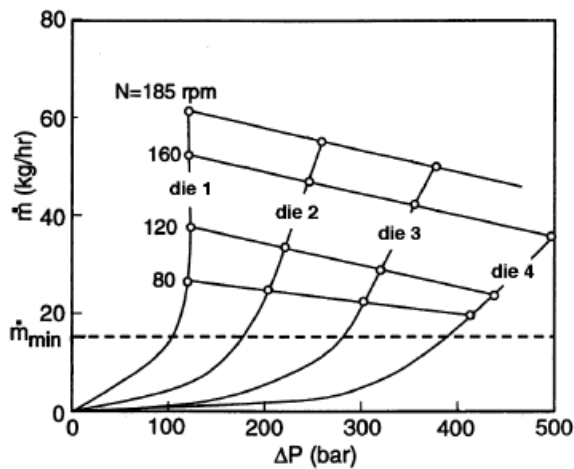


**Figure 6:** Die and screw characteristic pressure-throughput curves for LDPE in a  $D = 45$  mm extruder. Each open circle indicates the operating point for a die-rpm combination. [1]

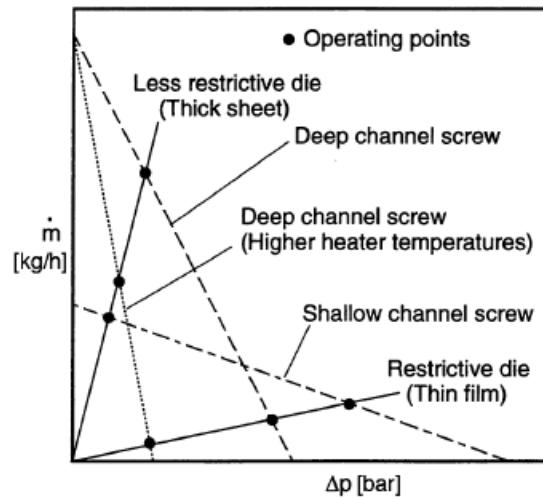


**Figure 7:** Screw and die characteristic pressure-throughput curves for a Newtonian fluid in an extruder with different channel depths. [1]

## 2.2 Twin extruders

Twin-screw extruders have been developed in particular for continuous mixing purposes compared to single screw extruders, latter are primarily used for high volume metering/pumping. In general, twin-screw extruders can be classified into counter-rotating and co-rotating twin-screw extruders, which are based on non-intermeshing, intermeshing, or close-intermeshing screws. These designs permit a wider range of possibilities in terms of output rate, mixing efficiency, heat generation, etc. In Figure 8 these types of extruders are schematically shown.



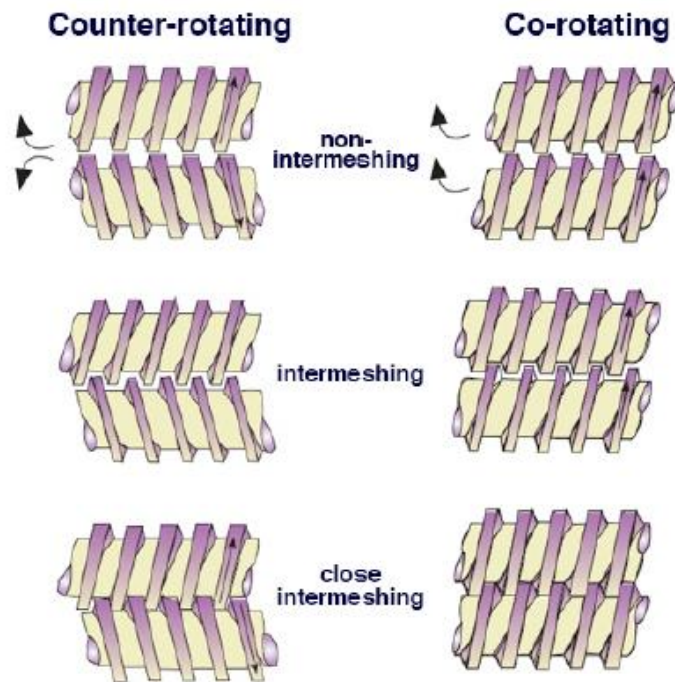


**Figure 8:** Design of different twin-screw

Most popular are co-rotating machines for efficient continuous mixing, including reactive extrusion. An intermeshing system is also self-cleaning. In summary, the co-rotating systems have a high pumping efficiency caused by the double transport action of two screws. This type of arrangement is particularly suitable for heat sensitive materials because the material is conveyed through the extruder with little possibility of entrapment. The counter-rotating systems generate high temperature pulses making them inappropriate for reactive extrusion, but they generate high stresses because of the calendaring action between screws, making them efficient machines to disperse pigments and lubricants. It is used commonly for powdered materials, particularly for rather temperature-sensitive PVC. The advantage of this extrusion system is the facilitated addition of polymer additives without stressing the material mechanically or thermally. This is important for polymers with solid constituents such as TiO<sub>2</sub>, mineral, clay, glass or fibers. It is also used for compounding techniques to prepare polymer blends by homogeneously mixing different polymers with a wide divergence in melting points (or glass transitions) and viscosities. Another advantage of this extrusion technique is a short retention time beneficial for temperature sensitive materials. If the generated pressure in the twin-screw extruder is not sufficiently high at the end of the metering zone, an additional melting pump can be added between the metering zone and the extrusion die. In contrast to the flood-feeding for single screw extruders, twin-screw extruders are operated in a starved-feeding mode. In this mode the polymer pellets, additives, fillers, or pigments are fed into the hopper by small amounts using gravimetric or volumetric screw feeders.

## References

1. T. A. Osswald, "Polymer Processing Fundamentals" Hanser-Verlag München 1998.
2. N. G. McCrum, C. P. Buckley, C. B. Bucknall, "Principles of Polymer Engineering" Oxford University Press, Oxford, 1997.
3. O. Schwarz, F.-W. Ebeling, B. Furth, "Kunststoffverarbeitung", 7. Aufl., Vogel Würzburg, 1997.
4. R. J. Crawford, "Plastics Engineering" 2nd Ed. Pergamon Press, Oxford 1987.
5. Lecture "Polymertechnologie", BSci PolKol, 6. Sem., Prof. V. Altstädt.
6. S. B. Brown, Annu. Rev. Mater. Sci. 21, 409-435 (1991).

## **(b) Thermal Characterization of Polymeric Materials**

### **Objective:**

The two major objectives of this experiment are as follows:

1. Study melting and crystalline transitions for various types of thermoplastics based on non-isothermal DSC measurements with different heating rates.
2. Calculate the glass transition temperature of various different types of thermosetting resins including epoxy, unsaturated polyester and vinyl ester.

### **Materials:**

PP and thermosetting polymers with and without any filler.

### **Equipment:**

Differential Scanning Calorimetry (DSC) with a finned air-cooling system (FACS).

## **1. Introduction**

Differential scanning calorimetry (DSC) is a technique used to investigate the response of polymers to heating. DSC can be used to study the melting of a crystalline polymer or the glass transition. The DSC set-up is composed of a measurement chamber and a computer. Two pans are heated in the measurement chamber. The sample pan contains the material being investigated. A second pan, which is typically empty, is used as a reference. The computer is used to monitor the temperature and regulate the rate at which the temperature of the pans changes. A typical heating rate is around  $10^{\circ}\text{C}/\text{min.}$ , the rate of temperature change for a given amount of heat will differ between the two pans. This difference depends on the composition of the pan contents as well as physical changes such as phase changes. For the heat flux DSC used in this lab course, the system varies the heat provided to one of the pans in order to keep the temperature of both pans the same. The difference in heat output of the two heaters is recorded, as shown in Figure 1.

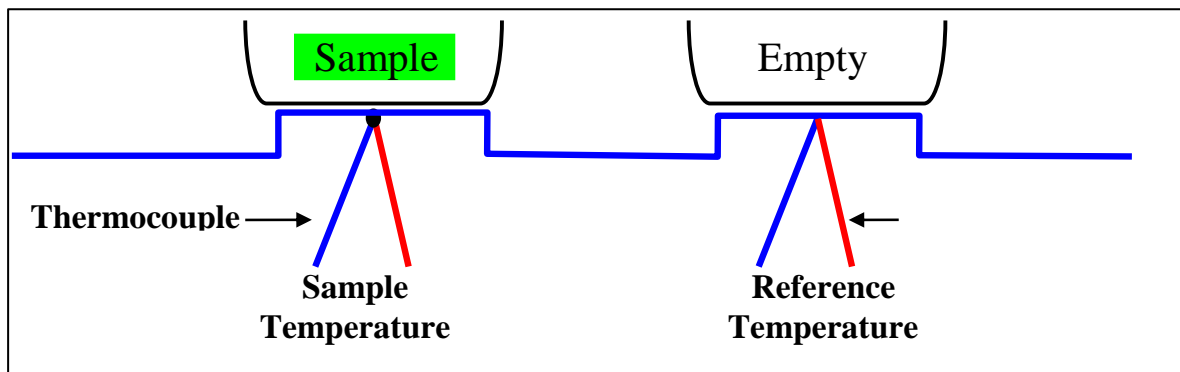


**Figure 1.** The simple illustration showing how DSC works.

The result is a plot of the difference in heat ( $q$ ) versus temperature ( $T$ ) **The heat capacity ( $C_p$ ) of a system** is the amount of heat needed to raise its temperature  $1^\circ\text{C}$ . It is usually given in units of  $\text{Joules}/^\circ\text{C}$  and can be found from the heat flow and heating rate. The heat flow is the amount of heat supplied per unit time.

$$\text{Heat flow} = \frac{\text{heat}}{\text{time}} = \frac{q}{t}$$

where  $t$  is time. The heating rate is the time rate change of temperature

$$\text{Heating rate} = \frac{\Delta T}{t}$$

Where  $\Delta T$  is the change in temperature. One can obtain the heat capacity from these quantities

$$C_p = \frac{\frac{q}{t}}{\frac{\Delta T}{t}} = \frac{q}{\Delta T}$$

This means the heat capacity can be found by dividing the heat flow by the heating rate. If the  $C_p$  of a material is constant over some temperature range, then the plot of heat flow against temperature will be a line with zero slopes as shown in Figure 2. If the heating rate is constant then the distance between the line and the x-axis is proportional to the heat capacity. If heat is plotted against temperature, then the heat capacity is found from the slope

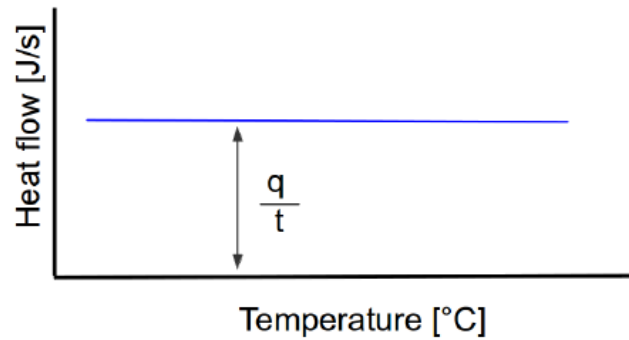


**Figure 2.** Example plot of heat flow versus temperature for a material that does not undergo any changes during the heating.

### 1.1. Glass Transition

If a polymer in its molten state is cooled it will at some point reach its glass transition temperature ( $T_g$ ). At this point the mechanical properties of the polymer change from those of an elastic material to those of a brittle one due to changes in chain mobility. A typical example of a heat flow versus temperature plot at a glass transition temperature is shown in Figure 3. The heat capacity of the polymer is different before and after the glass transition temperature. The heat capacity  $C_p$  of polymers is usually higher above  $T_g$ . DSC is a valuable method to determine  $T_g$ . It is important to note that the transition does not occur suddenly at one unique temperature but rather over a range of temperatures. The temperature in the middle of the inclined region is taken as the  $T_g$ .

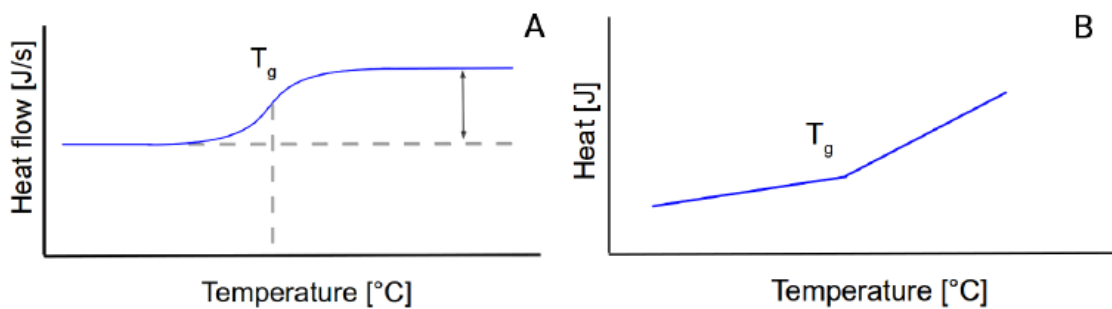


**Figure 3.** Schematics of a glass transition. The glass transition results in a kink in the heat versus temperature plot due to the change in heat capacity (A). In a plot of heat flow versus temperature, a gradual transition occurs over a range of temperatures (B). The glass transition temperature appears to be the middle of the sloped region.

## 1.2. Crystallization

Above the glass transition temperature the polymer chains have high mobility. At some temperature above  $T_g$  the chains have enough energy to form ordered arrangements and undergo crystallization. Crystallization is an exothermic process, so heat is released to the surroundings. Less heat is needed to keep the heating rate of the sample pan the same as that of the reference pan. This results in a decrease in the recorded heat flow. If the convention of 'exothermic - down' is used then the result is a dip in the plot of heat flow versus temperature as seen in Figure 4. Such a crystallization peak can be used to confirm that crystallization occurs in the sample and the crystallization temperature ( $T_c$ ) and determine the latent heat of crystallization. The crystallization temperature is called as the lowest point of the dip. The latent heat (enthalpy) of crystallization is determined from the area under the curve.

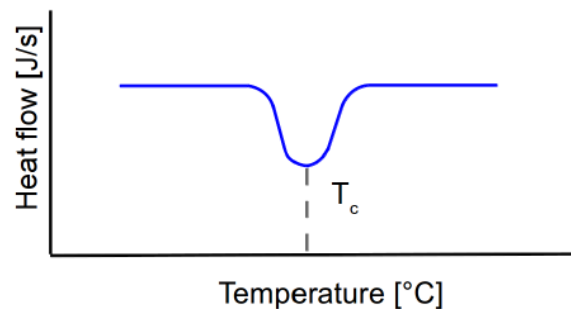


**Figure 4.** Example of a crystallization 'peak' in a plot of heat ow against temperature.

Crystallization is an exothermic process, so the heat ow to the sample must be decreased to maintain a constant heating rate.

## 1.3. Melting

The polymer chains are able to move around freely at the melting temperature ( $T_m$ ) and thus do not have ordered arrangements. Melting is an endothermic process, requiring the absorption of heat. The temperature remains constant during melting despite continued heating. The energy added during this time is used to melt the crystalline regions and does not increase the average kinetic energy of the chains that are already in the melt. In a plot of heat against temperature this appears as a jump discontinuity at the melting point as seen in Figure 5A. The heat added to the system during the melting process is the latent heat of melting. It can be calculated from the area of a melting peak observed in a plot of heat flow against temperature, such as the one in such as the one in Figure 5B. The  $T_m$  is called as the temperature at the peak apex. After melting the temperature again increases with heating. However, the heat capacity of a polymer in the melt is

higher than that of a solid crystalline polymer. This means the temperature increases at a slower rate than before.

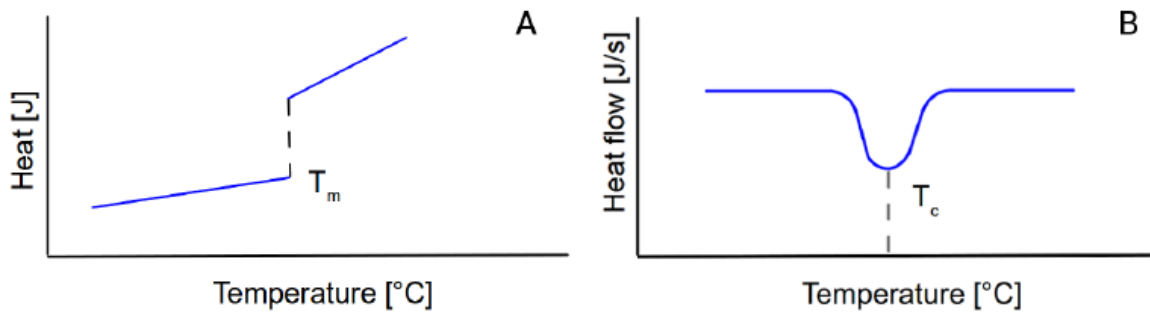


**Figure 5.** Melting is an endothermic process so the heat ow to the sample must be increased to keep the heating rate constant, resulting in a discontinuity in the plot of heat versus temperature (A). This appears as a peak if the heat ow is plotted against temperature (B). The area under the curve can be used to calculate the latent heat of melting.

An example of a DSC plot showing a glass transition, crystallization peak and melting peak is shown in Figure 6. It is worth noting that not all polymers undergo all three transitions during heating. The crystallization and melting peaks are only observed for polymers that can form crystals. While purely amorphous polymers will only undergo a glass transition, crystalline polymers typically possess amorphous domains and will exhibit a glass transition as seen in Figure 6. The amorphous portion only undergoes the glass transition while the crystalline regions only undergo melting. The exact temperatures at which the polymer chains undergo these transitions depend on the structure of the polymer. Subtle changes in polymer structure can result in huge changes in  $T_g$ .

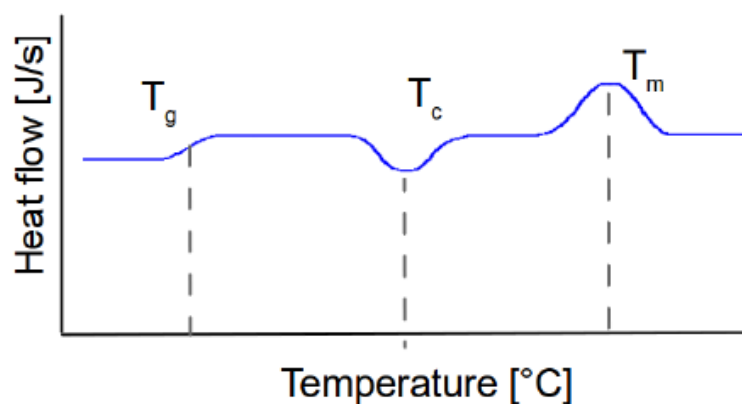


**Figure 6.** Example plot of a heat ow versus temperature plot for a polymer that undergoes as glass transition, crystallization and melting.

## **2. Experimental Procedure**

This experiment is divided into two separate parts. The first part involves using the DSC to study transitions in thermoplastic materials. For this purpose, different types of thermoplastic polymers are tested at heating rate of 5°C/ min. Note that non-isothermal DSC approach involves heating and cooling the material at constant heating rates to study the transitions. The second part involves determination of glass transition temperature ( $T_g$ ) of various types of thermosetting resins, including epoxy, unsaturated polyester and vinyl ester. For this purpose, the solid polymer samples are tested based on the procedure of heat-cool-heat cycle. Regardless of type of polymers or heating rates, all the measurements are carried out under nitrogen atmosphere with a flow rate of 50 ml/min.

### ***2.1 Sample preparation***

Weigh the aluminum pan using an analytical balance. Tare it, load it with the sample of interest and reweigh. During this course of action, you are required to handle the aluminum sample pans with forceps to avoid contamination of the sample. In common, sample weight loaded onto the DSC pan varies between 5 and 20 mg. In practice, smaller and larger sample sizes are to be, respectively, used at higher and slower heating rates to minimize thermal gradient in the sample upon heating and cooling. After loading the sample onto the pan, crimp the pan using the special tool. Check for flat pan bottom after crimping.

### ***2.2 Report Requirements***

1. Once the heating cycle of the thermoplastic samples is complete, report the followings.

Start and stop temperatures, onset temperature, peak maximum temperature (melting point) and peak area (heat of transition)

2. Once the subsequent cooling cycle of the thermoplastic samples is complete, report the followings.

Onset temperature, peak maximum temperature (crystallization point) and peak area (heat of transition).

3. Indicate  $T_g$  of the polymers.

## **References**

1. Barton, J. M. (1983), *Thermochim. Acta* 71, 337 – 344.
2. Barton, J. M. (1985), *Adv. Polym. Sci.* 72, 111 – 154.



3. Bates, F. S. and Fredrickson, G. H. (1990), *Annu. Rev. Phys. Chem.* 41, 525.
4. Beatty, C. L. and Karasz, F. E. (1979), *J. Macromol. Sci., Rev. Macromol. Chem. C* 17, 37.
5. Bilyeu, B. and Brostow, W. (2002), *Polym. Compos.* 23, 1111.
6. Blaine, R. L. and Marcus, S. M. (1998), *J. Therm. Anal.* 54, 467.

## **Experiment # 6: Thin Film Deposition and Characterization**

**Objective:** The objective is to learn thin film deposition processes and the main important parameters effecting thin film properties and how to determinate thin film properties (e.g. thickness, surface morphology, electrical resistance) via characterization techniques as Atomic Force Microscopy (AFM), X-Ray Reflectometry (XRR) and Four Point Probe (FPP).

**Materials:** Chemicals (ethanol, propanol, acetone, distilled water), Substrates (Si wafer, glass slide, fused silica, Quartz, flexible polymers), Targets (Metal, metal oxide etc.)

**Equipment:** Sputter System, Atomic Force Microscopy, X-Ray Reflectometry, Four Point Probe

### **Background:**

Thin films are fabricated by the deposition of individual atoms on a substrate. Thin film is defined as a low-dimensional material created by condensing, one-by-one, atomic/molecular/ionic species of matter. The thickness is typically less than several microns. Thin films differ from thick films. A thick film is defined as a low-dimensional material created by thinning a three-dimensional material or assembling large clusters/aggregates/grains of atomic/molecular/ionic species. Historically, thin films have been used for more than a half century in making electronic devices, optical coatings, instrument hard coatings, and decorative parts. High technology thin film applications include multilayer metal and insulating films in microelectronics, compound semiconductor films in optoelectronics, dielectric-film stacks for optical coatings, and ceramic film layers in hard coatings [1].

In all deposition techniques and application of thin films the vacuum technologies are imperative. Virtually every thin-film deposition and processing method or technique employed to characterize and measure the properties of films requires either a vacuum or some sort of reduced-pressure ambient. For example, there are plasma discharges, sustained at reduced gas pressures, in which many important thin-film deposition and etching processes occur. Evacuated spaces are usually populated by uncharged gas atoms and molecules [1]. The pressure scale is arbitrarily subdivided into corresponding low, medium, high, and ultrahigh vacuum domains, each characterized by different requirements with respect to vacuum hardware (e.g., pumps, gauges, valves, gaskets, feed throughs). Of the film deposition processes, evaporation requires a vacuum mainly in ultrahigh regimes, whereas sputtering between the high and low-pressure and

chemical vapour depositions are accomplished at the border between the medium and high vacuum ranges. Oil diffusion, turbo molecular, cryo-, and ion pumps produce the low pressures, while rotary, Roots, and sorption pumps are necessary to provide the necessary fore pressure for operation of the former [1].

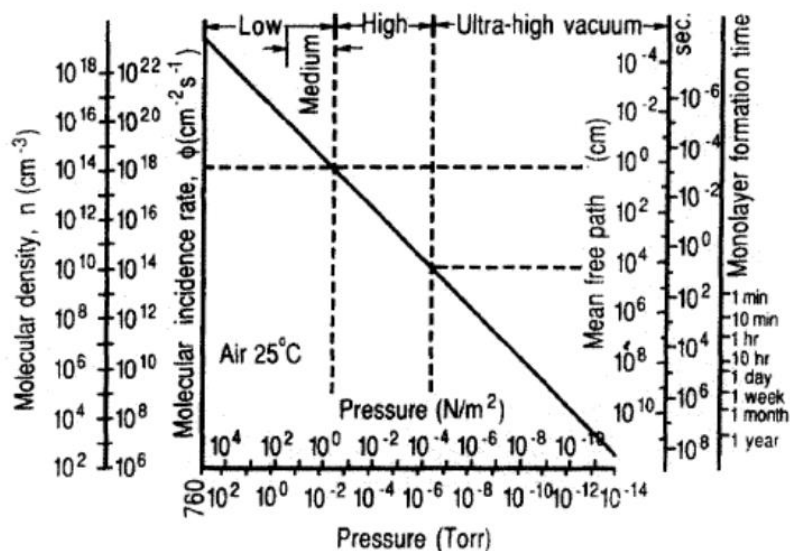


**Figure 1.** Molecular density, incidence rate, mean free path, and monolayer formation time as a function of pressure.

### **Thin Film Formation**

Any thin-film deposition process involves **three main steps**: 1. Production of the appropriate atomic, molecular, or ionic species. 2. Transport of these species to the substrate through a medium. 3. Condensation on the substrate, either directly or via a chemical and/or electrochemical reaction, to form a solid deposit.

**The Steps in Film Formation:** 1. Thermal accommodation; 2. Binding; 3. Surface diffusion; 4. Nucleation; 5. Growth; 6. Coalescence; 7. Continued growth. Depending on thermodynamic parameters of the deposit and the substrate surface, the initial nucleation and growth stages (4 and 5) of the many observations of film formation have pointed to three basic growth modes may be described as (a) island type, called Volmer-Weber type, (b) layer type, called Frank-van der Merwe type, and (c) mixed type, called Stranski-Krastanov type [2]. These are illustrated schematically in Fig.2. Island growth occurs when the smallest stable clusters nucleate on the substrate and grow in three dimensions to form islands. This happens when atoms or molecules in the deposit are more strongly bound to each other than to the substrate. Many systems of metals on insulators, alkali halide crystals, graphite, and mica substrates display this mode of growth [3]. The opposite characteristics are displayed during layer growth. Here the extension of the smallest stable nucleus occurs overwhelmingly in two dimensions resulting in the formation of

planar sheets. In this growth mode the atoms are more strongly bound to the substrate than to each other. The first complete monolayer is then covered with a somewhat less tightly bound second layer. Providing the decrease in bonding energy is continuous toward the bulk crystal value, the layer growth mode is sustained [3].

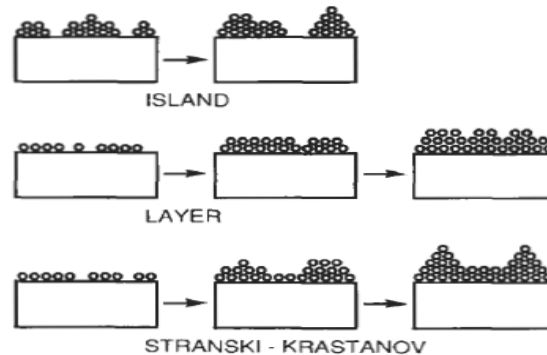


**Figure 2.** Thin film growth modes.

The layer plus island or Stranski-Krastanov growth mechanism is an intermediate combination of the aforementioned modes. In this case, after forming one or more mono layers, subsequent layer growth becomes unfavorable and islands form. The transition from two- to three-dimensional growth is not completely understood, but any factor that disturbs the monotonic decrease in binding energy characteristic of layer growth may be the cause. For example, due to film-substrate lattice mismatch, strain energy accumulates in the growing film. When released, the high energy at the deposit-intermediate layer interface may trigger island formation. This growth mode is fairly common and has been observed in metal-metal and metal-semiconductor systems [3].

### ***Thin Film Deposition Techniques***

Typical deposition processes are physical and chemical. The physical process is composed of the physical vapour deposition (PVD) processes, and the chemical processes are composed of the chemical vapour deposition (CVD) process (Fig. 3.).

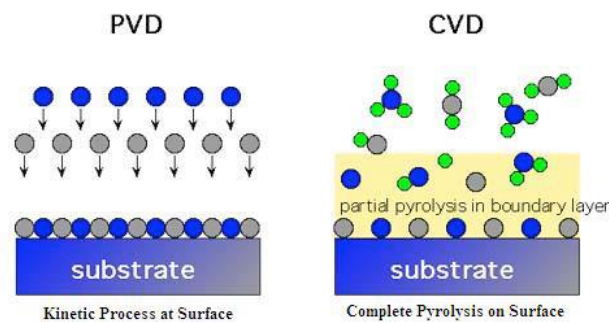


**Figure 3.** Schematic representation of physical and chemical vapor deposition.

In particular by the necessity to deposit insulating and passivating films, the CVD is served as a powerful processing method. PVD processes (often just called thin film processes) are atomistic deposition processes in which material is vaporized from a solid or liquid source in the form of atoms or molecules, transported in the form of a vapour through a vacuum or low pressure gaseous (or plasma) environment to the substrate where it condenses. Typically, PVD processes are used to deposit films with thicknesses in the range of a few nanometers to micrometers; however they can also be used to form multilayer coatings, graded composition deposits, very thick deposits and freestanding structures. The substrates can range in size from very small to very large such as the 10" x 12" glass panels used for architectural glass. The substrates can range in shape from flat to complex geometries such as watchbands and tool bits. Typical PVD deposition rates are 10–100Å (1–10 nanometers) per second. PVD processes can be used to deposit films of elements and alloys as well as compounds using reactive deposition processes. The main categories of PVD processing are thermal evaporation, sputter deposition, ion plating and arc vapour deposition.

### ***Sputtering Process***

For convenience sputtering processes are divided into four major categories: namely, DC, RF and magnetron. Magnetron sputtering is practiced in DC and RF as well as reactive variants and has significantly enhanced the efficiency of these processes. Sputter deposition utilizes an electrically excited gas plasma in a vacuum system. The ions in the plasma are accelerated toward the cathode, which upon bombardment eject neutral atoms from the cathode surface. The ejected atoms collect on all surfaces including the substrate surface [4]. Mainly sputtering process described in fig. 4. [1].

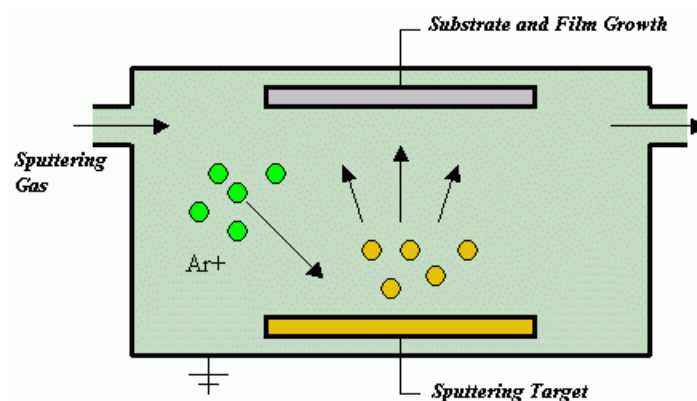


**Figure 4.** Sputtering Principle.

Magnetron sputtering applies a magnetic field around the target in order to energize argon atoms for bombarding the target. Using a magnetic field leads to trapping electrons in the magnetic field created around the target which enhances plasma. This results in higher ionization of argon atoms and bombarding rate that finally increases deposition rate [5].

### ***Thin Film Characterization Techniques***

The measurement of thin film properties is indispensable for the study of thin-film materials and devices. The chemical composition, crystalline structure, and optical, electrical, and mechanical properties must be considered in evaluating thin films [2]. Experimental techniques and applications associated with determination of “film thickness”, “film surface morphology and structure”, “film and surface composition”, “electrical properties of films”. These represent the common core of information required of all films and multilayer coatings irrespective of ultimate application.

***Atomic Force Microscope (AFM):*** The Atomic Force Microscope (AFM), which is sometimes called the Scanning Force Microscope (SFM), is based on the forces experienced by a probe as it approaches a surface to within a few angstroms. A typical probe has a 500 Å radius and is mounted on a cantilever which has a spring constant less than that of the atom-atom bonding. This cantilever spring is deflected by the attractive van der Waals (and other) forces and repulsed as it comes into contact with the surface (“loading”). The deflection of the spring is measured to within 0.1 Å. By holding the deflection constant and monitoring its position, the surface morphology can be plotted. Because there is no current flow, the AFM can be used on electrically conductive or non- conductive surfaces and in air, vacuum, or fluid environment.

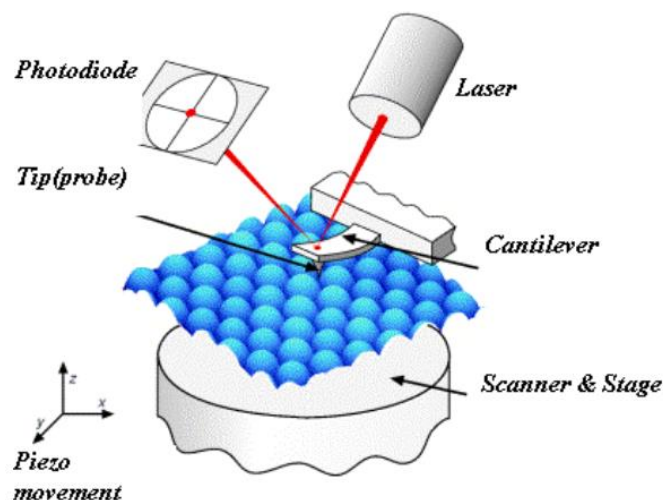


**Figure 5.** Schematic illustration of AFM. The tip is attached to a cantilever, and is scanned a surface. The cantilever deflection due to tip-surface interactions is monitored by a photodiode sensitive to laser light reflected at the tip backside [7].

The AFM can be operated in three modes: contact, noncontact and “tapping.” The contact mode takes advantage of van der Waal’s attractive forces as surfaces approach each other and provides the highest resolution. In the non-contacting mode, a vibrating probe scans the surface at a constant distance and the amplitude of the vibration is changed by the surface morphology. In the tapping mode, the vibrating probe touches the surface at the end of each vibration exerting less pressure on the surface than in the contacting mode. This technique allows the determination of surface morphology to a resolution of better than 10 nm with a very gentle contacting pressure (Phase Imaging) [6].

**Four Point Probe(FPP):** The purpose of the 4-point probe is to measure the resistivity or average resistance of a thin layer or sheet or any semiconductor material by passing current through the outside two points of the probe and measuring the voltage across the inside two points (see Fig. 6.).

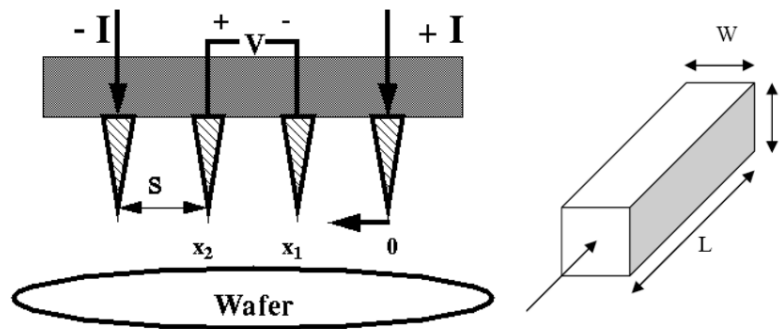


**Figure 6.** A view of FPP measuring geometry:  $x_1$  and  $x_2$  are positions,  $s$  is distance between probes.

### **Sheet resistance measurement principles**

The resistance  $R$  of a rectangular block of uniform bulk resistivity is given by:

$R = \rho \times L / A$ , where  $A = t \times W$  and  $\rho$ : resistivity of the sample.

$R = (\rho / t) \times (L / W) = R_s \times (L / W)$ , where  $R_s$ : sheet resistance of a layer of this material.

The sheet resistance is expressed in Ohm.square though strictly speaking it should be in Ohm.  $R_s$  can be determined by four probe measurement by applying a DC current in between the 2 outer current probes and measuring the voltage at the 2 inner voltage probes:  $R_s = V/I \times CF$ . The correction factor  $CF$  is dependent on the sample size and shape.

**X-Ray Reflectometry (XRR):** Most technological applications of thin films require films of definite thickness. This is because most properties of thin films are thickness dependent. Hence, determination of film thickness with high precision is very crucial for these technologies. XRR is a non-destructive and non-contact technique for thickness determination between 2-200 nm

with a precision of about 1-3Å. In addition to thickness determination, this technique is also employed for the determination of density and roughness of films and also multilayers with a high precision [8].

XRR method involves monitoring the intensity of the x-ray beam reflected by a sample at grazing angles. A monochromatic X-ray beam of wavelength  $\lambda$  irradiates a sample at a grazing angle  $\omega$  and the reflected intensity at an angle  $2\theta$  is recorded by a detector, see figure 7.

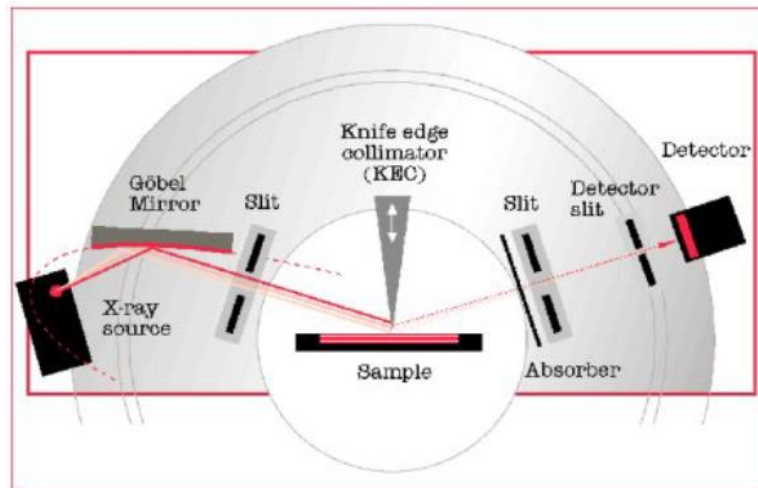


**Figure 6.** Schematic illustration of XRR measurement.

### Experimental Procedure

- Preparation and loading of substrate
- Thin film deposition by magnetron sputtering
- Morphological analysis by Atomic Force Microscopy
- Electrical analysis by Four Point Probe
- Thickness, roughness and density determination via X-ray reflectivity method

### References

1. Ohring, M., Material Science of Thin Films Deposition & Structure Second Edition, Academic Press, USA, 2002.
2. Wasa, K., Kitabatake, M., Adachi H., Thin Film Materials Technology Sputtering of Compound Materials, William Andrew Publishing, USA, 2004.
3. Ohring, M., The Materials Science of Thin Films First Edition, Academic Press, USA, 1992.



4. Sarangan, A., & Haus, J. W. (2016). Quantum mechanics and computation in nanophotonics. *Fundamentals and applications of nanophotonics*. Woodhead Publishing, 45-87.
5. Low, I. M. (Ed.). (2012). Advances in science and technology of  $Mn^{+1}AX_n$  phases.
6. Mattox, Donald M., Handbook of Physical Vapor Deposition (PVD) Processing Film Formation, Adhesion, Surface Preparation and Contamination Control, Noyes Publication, USA, 1998.
7. <http://www.farmfak.uu.se/farm/farmfyskem-web/instrumentation/afm.shtml>
8. <http://ia.physik.rwth-aachen.de/methods/xray/www-xray-eng.pdf>

## **Experiment # 7: Fatigue, Charpy Impact and Tension Testing, Ndt Experiments**

### **(a) Fatigue, Charpy Impact and Tension Testing**

**Objective:** The objective of the Charpy impact experiment is to evaluate the energy absorbing characteristics of metal materials at room temperature using the Charpy impact method. The object of the fatigue test is to comprehend how fatigue conditions affect metals and to determine the fatigue life of the specimen. The object of the tension testing is to determine the tensile properties for various metallic samples using the American Standard Test Methods (ASTM).

**Materials:** *V-notch* Charpy impact samples. Fatigue samples. A set of metallic specimens prepared according to the tension testing standards.

**Equipment:** Impact testing machine for Charpy impact test. Instron Universal Testing Machine for fatigue and tension tests.

### **Background:**

#### **1. Charpy Impact Test**

Charpy impact test is a method for evaluating the toughness and notch sensitivity of engineering materials. It is used to test the toughness of metals, but similar tests are used for polymers, ceramics and composites. The test measures the energy absorbed by the fractured specimen. This absorbed energy is a measure of a given material's toughness. Charpy impact testing involves striking a standard notched specimen with a controlled weight pendulum swung from a set height. The standard Charpy-V notch specimen is 55mm long, 10mm square and has a 2mm deep notch with a tip radius of 0.25mm machined on one face (Figure 1)

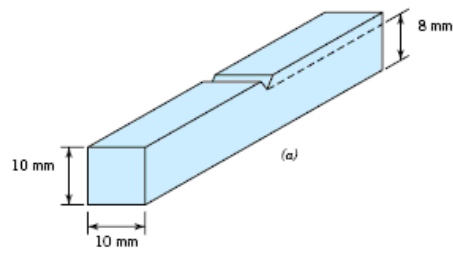


**Figure 1.** Standard specimen for Charpy Impact Test

The specimen is supported at its two ends on an anvil and struck on the opposite face to the notch by the pendulum (Figure 2). The amount of energy absorbed in fracturing the test-piece is measured and this gives an indication of the notch toughness of the test material. The pendulum swings through during the test, the height of the swing being a measure of the amount of energy absorbed in fracturing the specimen.

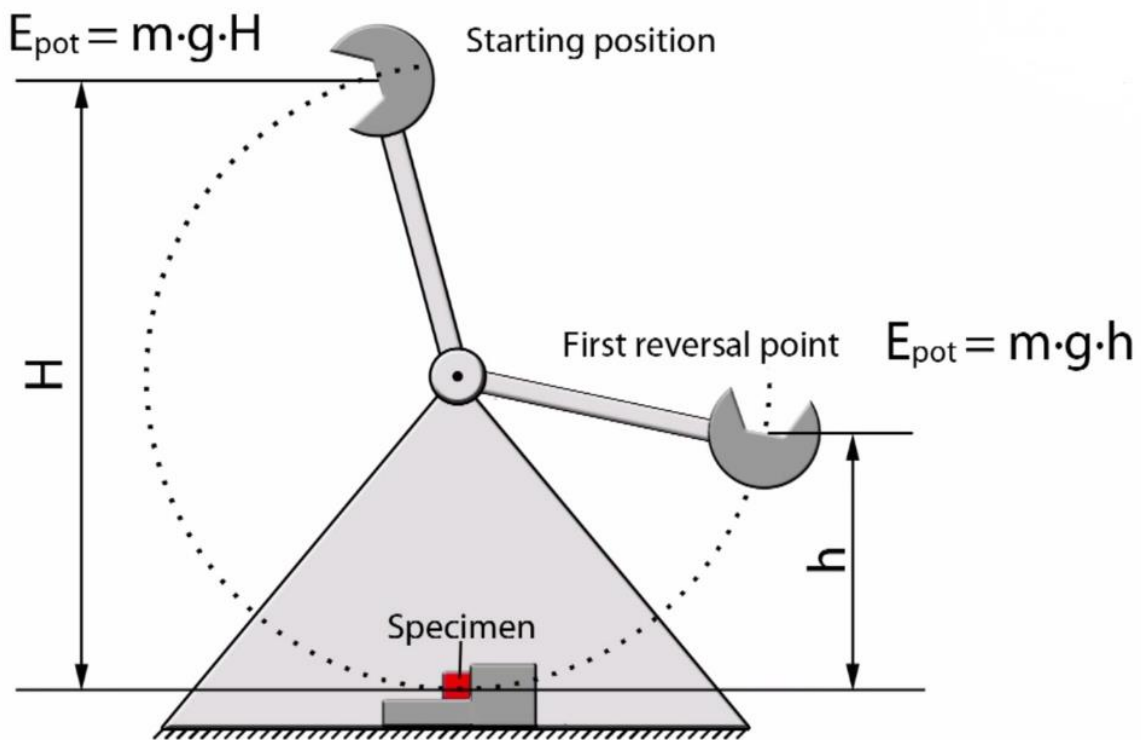


**Figure 2.** Charpy Impact Test (1)

Charpy tests show whether a metal can be classified as being either brittle or ductile. This is particularly useful for ferritic steels that show a ductile to brittle transition with decreasing temperature. A brittle metal will absorb a small amount of energy when impact tested, a tough ductile metal absorbs a large amount of energy. The appearance of a fracture surface also gives

information about the type of fracture that has occurred; a brittle fracture is bright and crystalline, a ductile fracture is dull and fibrous. The percentage crystallinity is determined by making a judgement of the amount of crystalline or brittle fracture on the surface of the broken specimen, and is a measure of the amount of brittle fracture.

## Experimental Procedure

1. Pulling the pendulum at a known height and engaging the safety latch
2. Clamping the specimen in the machine
3. Releasing the pendulum
4. Reading the result from the indicator

## 2. Fatigue Testing

### Introduction:

In many applications, materials are subjected to vibrating or fluctuating forces. The behavior of materials under such load conditions differs from the behavior under a static load. Designers are faced with predicting fatigue life, which is defined as the total number of cycles to failure under specified loading conditions, since the material is subjected to repeated load cycles (fatigue) in actual use. Fatigue testing data is used to predict cycle number of crack initiation and crack propagation behavior.

### Test specimen

The fatigue test specimen is center crack tension (CCT) type and was made by 2024-T3 aluminum alloy. The width ( $W$ ), length ( $L$ ) and thickness ( $B$ ) of the specimens are 90, 300, 6 mm, respectively. The specimen was machined according to ASTM E 647 recommendation (Figure 1).

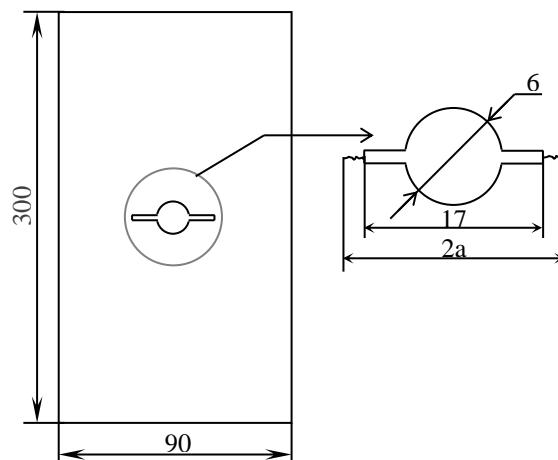


**Figure 1.** The fatigue crack growth CCT specimen geometry (dimensions mm).

## **Experimental Procedure**

1. Selecting test parameters and calculating maximum and average load values
2. Clamping the specimen
3. Inputting test parameters to the MAX program controlling the test machine
4. Starting the test
5. Monitoring and measuring the crack length by the traveling microscope.

## **3. Tensile Testing**

### ***Introduction***

A tensile test is probably the most fundamental type of mechanical test you can perform on material. Tensile tests are simple, relatively inexpensive, and fully standardized. By pulling standard specimens you will very quickly determine how the material will react to forces being applied in tension. As the material is being pulled, you will find its strength along with how much it will elongate. Data from test are used to determine *elastic limit, elongation, modulus of elasticity, proportional limit, and reduction in area, tensile strength, yield point, yield strength* and other tensile properties. Procedures for tension tests of metals are given in ASTM E-8. Methods for tension tests of plastics are outlined in ASTM D-638, ASTM D-2289 (high strain rates), and ASTM D-882 (thin sheets).

### ***Why Perform a Tensile Test or Tension Test?***

You can learn a lot about a substance from tensile testing. As you continue to pull on the material until it breaks, you will obtain a good, complete tensile profile (Figure 1). A curve will result showing how it reacted to the forces being applied. A stress-strain test typically takes several minutes to perform and is destructive; that is, the test specimen is permanently deformed and usually fractured. The point of failure is of much interest and is typically called its "**Ultimate Strength**" or UTS on the chart (Figure 1).

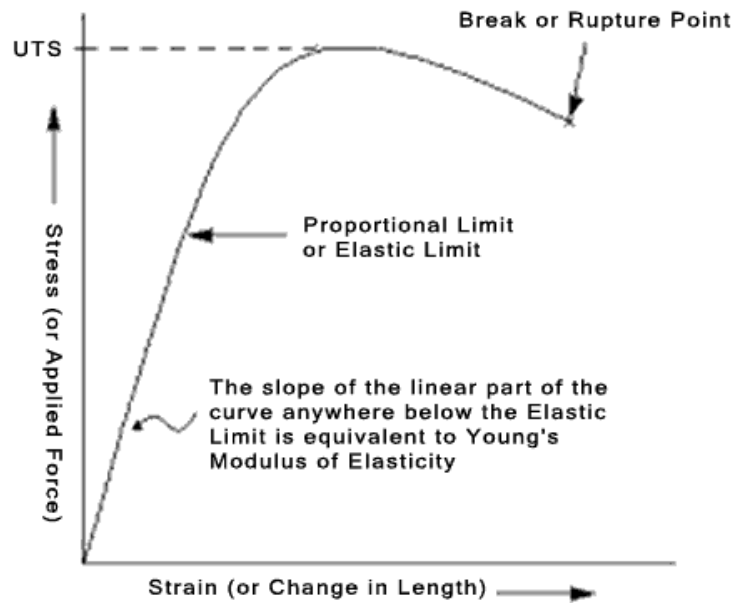


**Figure 1.** Tensile testing profile for metallic materials (3)

**Hooke's Law** for most tensile testing of materials, you will notice that in the initial portion of the test, the relationship between the applied force, or load, and the elongation the specimen exhibits is linear (Figure 2). In this linear region, the line obeys the relationship defined as "Hooke's Law" where the ratio of stress to strain is a constant, or  $\frac{\sigma}{\epsilon} = E$ .  $E$  is the slope of the line in this region where stress ( $\sigma$ ) is proportional to strain ( $\epsilon$ ) and is called the "**Modulus of Elasticity**" or "**Young's Modulus**".

### ***Modulus of Elasticity***

The modulus of elasticity is a measure of the stiffness of the material, but it only applies in the linear region of the curve. If a specimen is loaded within this linear region, the material will return to its exact same condition if the load is removed. At the point that the curve is no longer linear and deviates from the straight-line relationship, Hooke's Law no longer applies and some permanent deformation occurs in the specimen. This point is called the "elastic, or **proportional, limit**". From this point on in the tensile test, the material reacts plastically to any further increase in load or stress. It will not return to its original, unstressed condition if the load were removed.

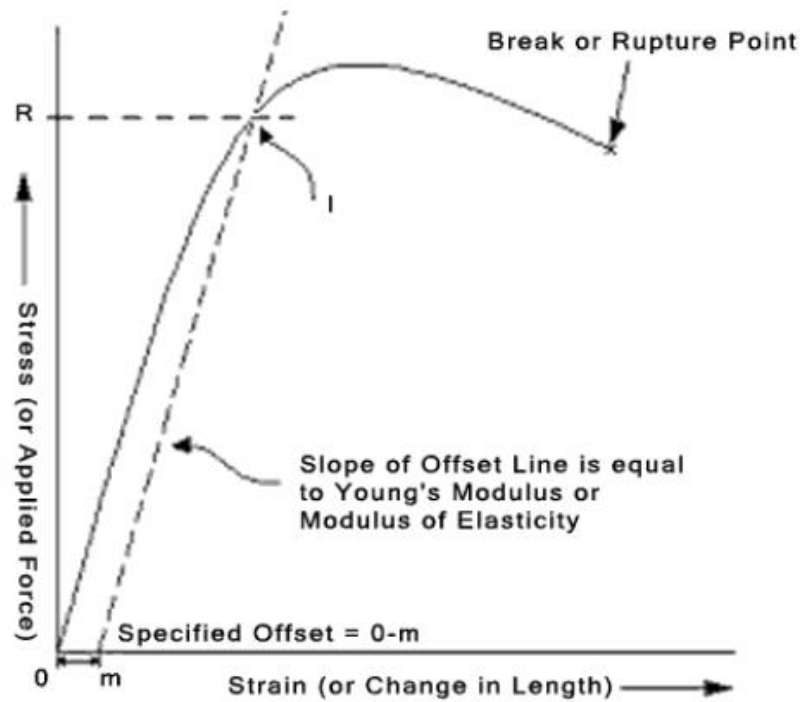


**Figure 2.** The linear portion of stress-strain curve (3)

### *Yield Strength*

A value called "**yield strength**" of a material is defined as the stress applied to the material at which plastic deformation starts to occur while the material is loaded.

### *Strain*

You will also be able to find the amount of stretch or elongation the specimen undergoes during tensile testing. This can be expressed as an absolute measurement in the change in length or as a relative measurement called "strain". Strain itself can be expressed in two different ways, as "engineering strain" and "true strain". Engineering strain is probably the easiest and the most common expression of strain used. It is the ratio of the change in length to the original length,

$$e = \frac{L - L_0}{L_0} = \frac{\Delta L}{L_0}.$$

Whereas, the true strain is similar but based on the instantaneous length of the specimen as the test progresses, where  $L_i$  is the instantaneous length and  $L_0$  the initial length.

$$\epsilon = \ln\left(\frac{L_i}{L_0}\right)$$

### **Experimental Procedure**

We will serve to introduce the Instron testing equipment and testing procedures. For the experiment, a 8 mm nominal diameter hot rolled steel sample will be tested to failure. Load versus- strain diagrams will be produced during the test and this diagram will subsequently be used to determine material properties. The student will learn how to properly conduct a tension test and obtain the relevant material properties from the results. Further, the student will discover how different materials behave under similar loading conditions as well as how material properties differ.

### **Report Requirements**

For the material tested please determine and tabulate the following properties:

- a. Proportional Limit
- b. Yield Strength
- c. Ultimate Strength
- d. Modulus of Elasticity
- e. Percent elongation
- f. Percent reduction in area
- g. Provide stress versus strain plot, appropriately labeled, for specimen tested
- h. Briefly summarize, in words, tension test.

### **REFERENCES**

1. <http://www.fabbaloo.com/blog/2014/6/15/design-of-the-week-diy-material-testing-machine>
2. William D. Callister, Jr. (2007) An Introduction: Materias Science and Engineering (Seventh Edition), United States of America
3. <http://www.instron.com.tr/tr-tr/our-company/library/test-types/tensile-test>
4. Michael F Ashby& David R H Jones (1980), Engineering Materials 1, Pergamon Press



## (b) Non-Destructive Testing (NDT)

**Objective:** To introduce the use and the importance of non-destructive testing methods.

**Materials:** Aircraft landing gear, wings and fuselage parts

**Equipment:** Dye Penetrant, Ultrasonic Testing, Magnetic Particle Testing and Eddy Current Testing equipments

### Background:

Non-destructive tests (NDT) are inspection methods which are usually used to search for the presence of defects in components, without causing any effects on the properties of the components. The types of defects detectable are cracks, porosity, voids, inclusions, etc.

Modern NDT is used by manufacturers to: ensure product integrity and reliability; prevent failure, accidents and saving lives; make profit for users; ensure customer satisfaction; aid in better product design; control manufacturing process; lower manufacturing costs; maintain uniform quality level; ensure operational readiness.

Table 1 shows the types of NDT methods used today.

**Table 1.** The types of NDT methods

Commonly Used Methods	Other Methods
Ultrasonics	Visual Methods
Radiography	Acoustic Emission
Dye Penetrant	Thermography
Magnetic Particle Inspection	Holography
Eddy Current	

### 1. Basic Principles of Ultrasonic Testing

Mechanical vibrations can propagate in solids, liquids and gases. The actual particles of matter vibrate, and if the mechanical movements of the particles have a regular motion, the vibration can be assigned a frequency in cycles per second, measured in hertz (Hz), where 1 Hz = 1 cycle per second. If this frequency is within the approximate range 10 to 20,000 Hz, the sound is audible; above about 20 kHz, "the sound" waves are referred to as **ultrasound or ultrasonics**.

The ultrasonic principle is based on the fact that solid materials are good conductors of sound waves. The waves are not only reflected at the interfaces but also by internal flaws (material separations, inclusions, etc.).

As an example of a practical application, if a disc of piezoelectric materials is attached to a block of steel (Figure 1a), either by cement or by a film of oil, and a high-voltage electrical pulse is applied to the piezoelectric disc, a pulse of ultrasonic energy is generated in the disc and is propagated into the steel. This pulse of waves travels through the metal with some spreading and some attenuation and will be reflected or scattered at any surface or internal discontinuity such as an internal flaw in the specimen. This reflected or scattered energy can be detected by a suitably-placed second piezoelectric disc on the metal surface and will generate a pulse of electrical energy in that disc. The time-interval between the transmitted and reflected pulse is a measure of the distance of the discontinuity from the surface, and the size of the return pulse can be a measure of the size of the flaw. This is the simple principle of the ultrasonic flaw detector and the ultrasonic thickness gauge. The piezoelectric discs are the "probes" or "transducers"; sometimes it is convenient to use one transducer as both transmitter and receiver. In a typical ultrasonic flaw detector the transmitted and received pulses are displayed in a scan on a timebase on an oscilloscope as shown in Figure 1b.

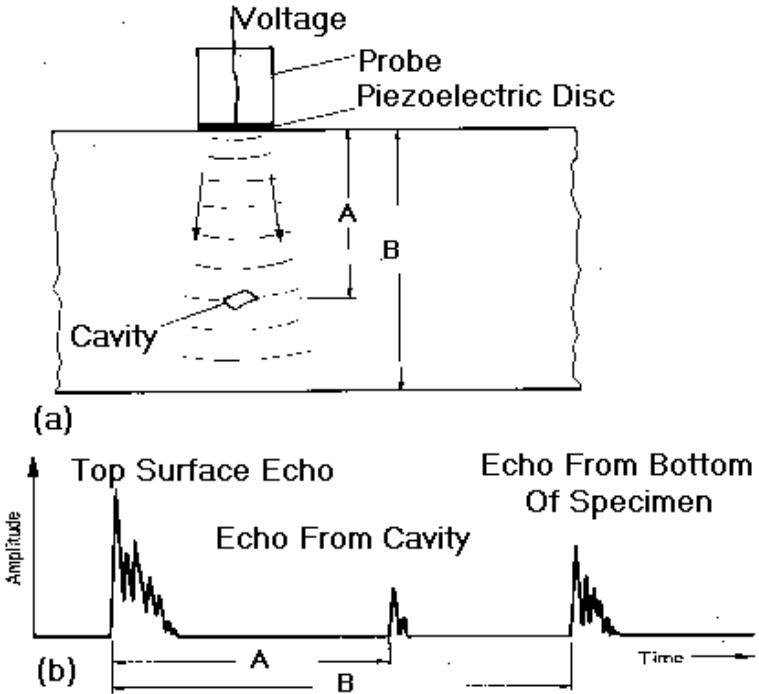


**Figure 1.** An example of practical application of ultrasonic testing methods a) Pulse b) Echo.

## 2. Radiography (Rt)

Radiography involves the use of penetrating gamma or X-radiation to examine parts and products for imperfections. This method is widely used for the detection of cracks and damage in aircraft structures (Figure 2). An X-ray generator or radioactive isotope is used as a source of radiation. Radiation is directed through a part and onto film or other imaging media. The resulting shadowgraph shows the dimensional features of the part. Possible imperfections are indicated as density changes on the film in the same manner as a medical X-ray shows broken bones.



**Figure 2.** Detection of cracks in aircraft structure by Radiography method.

## 3. Dye Penetrant

This method used to locate surface breaking flaws such as cracks, porosity, laps, seams and other surface discontinuities. Penetrant testing is used to test non-ferrous materials such as aluminum and stainless steel. Different test methods are available ranging from visible red/water washable penetrant systems to complex emulsifier penetrant systems. Various sensitivities are selected based on the product and customer requirements. The tested item is cleaned first before the penetrant is applied by dipping, spraying or brushing. The penetrant is given time to soak into any defects, the penetration time dependent on the chosen penetrant and customer requirement. Afterwards, the excess penetrant is removed and the component is dried depending on the process used. Then a developer is applied. The developer helps to draw the penetrant out of the flaw and onto the surface to form a visible indication (Figure 3). A visual inspection is then performed by the inspector under ultraviolet or white light, depending on the type of penetrant used (fluorescent or visible color contrast).

Common uses would be:

- Non-ferrous parts can readily be tested using this method
- Aircraft components
- Non-ferrous castings
- Finished machined components

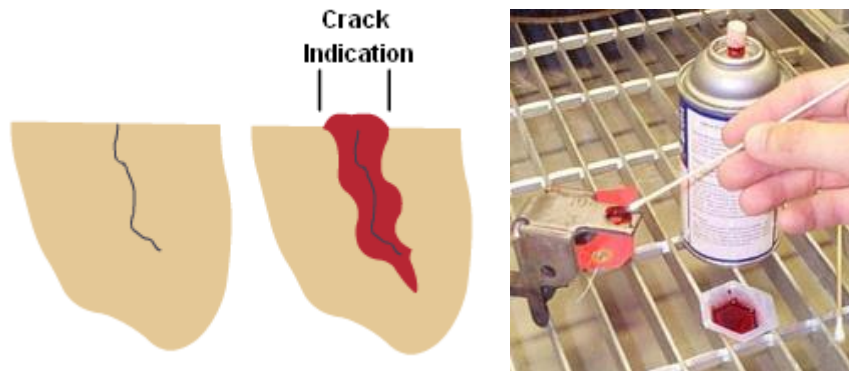


**Figure 3.** Detection of cracks by dye penetrant

#### 4. Magnetic Particle Testing (Mt)

This method is accomplished by inducing a magnetic field in a ferromagnetic material and then dusting the surface with iron particles (either dry or suspended in liquid). Surface and near-surface imperfections distort the magnetic field and concentrate iron particles near imperfections, providing a visual indication of the flaw (Figure 4).

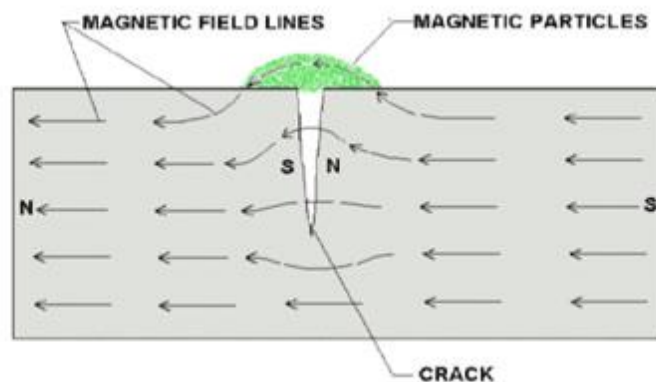


**Figure 4.** Application of Magnetic Particle testing method

#### 5. Electromagnetic Testing (Et) or Eddy Current Testing

Electrical currents are generated in a conductive material by an induced alternating magnetic field. The electrical currents are called eddy currents because they flow in circles at and just

below the surface of the material. Interruptions in the flow of eddy currents, caused by imperfections, dimensional changes, or changes in the material's conductive and permeability properties, can be detected with the proper equipment (Figure 5).

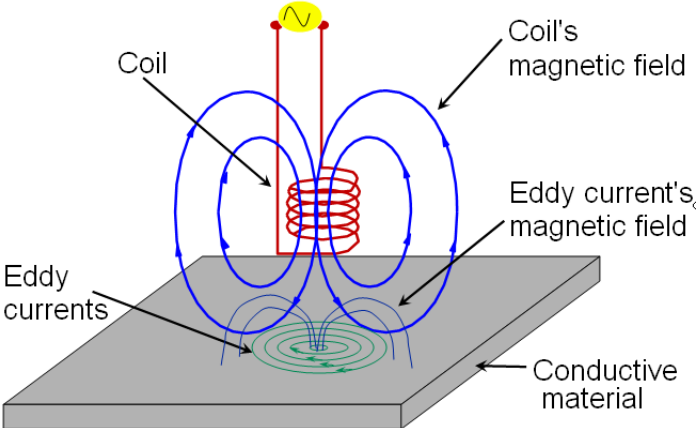


**Figure 5.** Crack detection by Eddy current testing method

**References**

1. [https://www.faa.gov/documentLibrary/media/Advisory\\_Circular/Chapter\\_05.pdf](https://www.faa.gov/documentLibrary/media/Advisory_Circular/Chapter_05.pdf)